Unveiling diverse clinical symptom patterns and neural activity profiles in major depressive disorder subtypes

Xiang Wang,[a,b,c,d,e,f] Yingying Su,[e,f,g] Qian Liu,[a,b,c,d] Muzi Li,[e,f,h,i] Yashar Zeighami,[j] Jie Fan,[a,b,c,d] G. Camelia Adams,[k] Changlian Tan,[l] Xiongzhao Zhu,[a,b,c,d,*] and Xiangfei Meng[e,f,m,**]

[a]Medical Psychological Center, The Second Xiangya Hospital of Central South University, Changsha, Hunan, China
[b]Medical Psychological Institute of Central South University, Central South University, Changsha, Hunan, China
[c]National Clinical Research Center on Mental Disorders (Xiangya), Changsha, Hunan, China
[d]National Center for Mental Disorder, Changsha, Hunan, China
[e]Department of Psychiatry, Faculty of Medicine and Health Sciences, McGill University, Montréal, QC, Canada
[f]Douglas Research Centre, Montréal, QC, Canada
[g]School of Public Health and Emergency Management, Southern University of Science and Technology, Shenzhen, Guangdong, China
[h]School of Mechanical and Electronic Engineering, Hubei Polytechnic University, Huangshi, Hubei, China
[i]Hubei Key Laboratory of Intelligent Conveying Technology and Device, Huangshi, Hubei, China
[j]Department of Neurology and Neurosurgery, Montreal Neurological Institute, McGill University, Montréal, QC, Canada
[k]Department of Psychiatry, University of Saskatchewan, Saskatoon, SK, Canada
[l]Department of Radiology, The Second Xiangya Hospital of Central South University, Changsha, Hunan, China
[m]Interdisciplinary School of Health Sciences, Faculty of Health Sciences, University of Ottawa, Ottawa, ON, Canada

eBioMedicine
2025;116: 105756
Published Online xxx
https://doi.org/10.1016/j.ebiom.2025.105756

Summary

Background The heterogeneity of major depressive disorder (MDD) significantly hinders its effective and optimal clinical outcomes. This study aimed to identify MDD subtypes by adopting a data-driven approach and assessing validity based on symptomatology and neuroimaging.

Methods A total of 259 patients with MDD and 92 healthy controls were enrolled in this cross-sectional study. Latent profile analysis (LPA) was used to identify MDD subtypes based on validated clinical symptoms. To examine whether there were differences between these identified MDD subtypes, network analysis was used to test any differences in symptom patterns between these subtypes. We also compared neural activity between these identified MDD subtypes and tested whether certain neural activities were related to individual subtypes. This MDD subtyping was further tested in an independent dataset that contains 86 patients with MDD.

Findings Five MDD subtypes with distinct depressive symptom patterns were identified using the LPA model, with the 5-class model selected as the optimal classification solution based on its superior fit indices (AIC = 6656.296, aBIC = 6681.030, entropy = 0.917, LMR $p = 0.3267$, BLRT $p < 0.001$). The identified subtypes include atypical-like depression, two melancholic depression (moderate and severe) subtypes with distinct patterns on *feeling anxious*, and two anhedonic depression subtypes (moderate and severe) with different manifestations on *weight/appetite loss*. The reproducibility of the classification was also confirmed. Significant differences in symptom structures between melancholic and two anhedonic subtypes, and between anhedonic and atypical subtypes were observed (all $p < 0.05$). Furthermore, these identified subtypes had differential neural activities in both regional spontaneous neural activity ($pFWE < 0.005$) and functional connectivity between different brain regions ($pFDR < 0.005$), linked to different clinical symptoms ($FDR\ q < 0.05$).

Interpretation The network analysis and neuroimaging tests support the existence and validity of the identified MDD subtypes, each exhibiting unique clinical manifestations and neural activity patterns. The categorisation of these subtypes sheds light on the heterogeneity of depression and suggest that personalised treatment and management strategies tailored to specific subtypes may enhance intervention strategies in clinical settings.

Funding National Natural Science Foundation of China (NSFC) and China Scholarship Council (CSC).

*Corresponding author. Medical Psychological Center, The Second Xiangya Hospital of Central South University, 139 Renmin Middle Road, Changsha, 410011, China.
**Corresponding author. Interdisciplinary School of Health Sciences, Faculty of Health Sciences, University of Ottawa, Ontario, Canada.
E-mail addresses: xiongzhaozhu@csu.edu.cn (X. Zhu), xiangfei.meng@uottawa.ca (X. Meng).

Keywords: Major depressive disorder; Clinical subtypes; Latent profile analysis; Symptom network structures; Neural activity; Resting-state fMRI

Research in context

Evidence before this study

The heterogeneity of major depressive disorder (MDD) significantly hinders its diagnosis, effective clinical management, and patient-centred recovery paths. Numerous studies have attempted to uncover this heterogeneity using data-driven approaches to classify MDD subtypes based on various sources of information, including symptomatology, medication response and multi-level biomarkers. However, clinical translation remains challenging because rich biological information is often difficult to obtain in clinical practice and may not be feasible for accurately distinguishing subtypes at the individual level. As a result, it is a challenge to implement findings of MDD biotypes in clinical practice, leaving ongoing challenges in fully unveiling the heterogeneity of MDD and its clinical translation.

Added value of this study

The current study provided a person-centred method to identify MDD subtypes at the individual level based on standard DSM depressive symptoms. Using this method, five subtypes with unique symptom patterns were identified, and the existence and validity of these identified MDD subtypes were verified at both the symptomatology and neurophysiology levels. Notably, the reproducibility of the classification was also confirmed in an independent dataset, demonstrating good generalisability. This work contributes to the literature by advancing the understanding of MDD heterogeneity through the identification of clinical subtypes characterised by distinct symptom patterns and unique associated neural activity alterations, and highlights their incremental value for clinical translation.

Implications of all the available evidence

These findings could help to address the challenges of clinical implementation faced by prior studies. By utilising accessible standard DSM depressive symptoms combined with the model generated by the current study, clinicians can more effectively identify patient subtypes. This enables clinicians to provide targeted and specialised treatments focussing on relevant therapeutic targets based on the neuroimaging characteristics of each subtype, thereby helping to yield optimal treatment outcomes.

Introduction

The heterogeneity of major depressive disorder (MDD) presents challenges for orientating individuals towards the treatment to which they are most likely to respond,[1] significantly hindering diagnosis, effective clinical management, and patient-centred recovery paths.[2,3] Earlier and more accurate identification of MDD subtypes can enable personalised treatment and management.[4–7] Most studies on MDD subtyping have utilised data-driven approaches to classify MDD subtypes based on symptomatology,[8–13] genetics,[14] neurotransmitter distributions,[15–17] medication response (e.g., netamiftide, ketamine),[18,19] as well as shared brain alteration signatures.[20–24] These pioneering works have initiated a novel but early stage of subtyping MDD.[22]

Studies utilising depressive symptoms to characterise MDD subtypes have generally identified three to five subtypes: atypical, melancholic,[25] seasonal,[26] psychotic,[27] and anxiety/agitated subtypes.[28,29] These discoveries, to some extent, have direct clinical implications,[30] with some evidence reporting that patients with melancholic MDD have shown a response to tricyclic antidepressants, whereas those with atypical MDD were more responsive to monoamine oxidase inhibitors.[31] However, most symptom-based studies, particularly those relying on statistical clustering of symptom profiles, have primarily identified subtypes that differed in severity rather than different symptom patterns,[8,10,11] which may be partially explained by the lack of inclusion of all of the Diagnostic and Statistical Manual of Mental Disorders (DSM) criterion symptoms. Furthermore, some studies attempting to distinguish DSM-defined melancholic or atypical subtypes have not provided further evidence to support the validity of the classification.[8–13]

Despite the promising emerging trend in recent years to use multiple data sources (e.g., data on symptomatology, genetic, biochemical, and neuroimaging, etc.) to identify MDD subtypes, these findings have shown substantial heterogeneity and inconsistency, and are often limited by restricted clinical relevance and a lack of validation and replication, limiting their clinical application, generalisability as well as the mechanistic insights they provide. Moreover, some studies have worked with a small sample size, which restricts the identification of MDD subtypes with subtle differences.[23,32] For instance, some studies were based on neurotransmitter distributions and found that there might be MDD subtypes with and without disturbed neurotransmitter levels.[15–17] However, little is known about how these identified subtypes are connected to clinical manifestations and outcomes. One study

attempted to use genetic information for subtyping and yielded an inconclusive answer on MDD subtypes due to its small sample size, limited choice of the studied genetic markers, and no replication study.[14] Others have utilised data on medication response (e.g., netamiftide, ketamine) to categorise MDD subtypes.[18,19] These studies either had a small sample size or limited biological relevance. More recent studies have tried to identify neurophysiological subtypes, or biotypes by clustering subjects according to shared signatures of brain alterations,[20–24,32,33] but the identified subtypes significantly differed between studies. For example, one study used functional magnetic resonance imaging (fMRI) data and unveiled two subtypes, but these two subtypes only had differences in symptom severity and duration.[24] A diffusion tensor imaging study only unveiled two distinct subtypes within different age groups (early onset vs. later onset), but the effects of age vs. age of onset could not be well distinguished because there were many first-episode subjects.[23] Drysdale et al.[22] and Dunlop et al.[33] discovered certain biotypes using fMRI which accounted for individual differences in clinical symptom profiles, holding promise in terms of clinical value. However, patients may not be able to directly benefit from these biologically-based subtyping findings in clinical practice, primarily due to the challenges associated with data accessibility and the high costs involved in acquiring such data.

In contrast, depressive symptoms are easier to assess in clinical settings, are more directly linked to clinical manifestations, and offer a more immediate means for informing personalised treatment strategies. Therefore, symptom-based subtyping, if rigorously validated, holds greater translational potential for improving clinical decision-making and management of MDD. Nonetheless, the methodological limitations of prior symptom-based subtyping studies have impeded progress towards this objective. To realise this potential, standardised and rigorously validated research on symptom-based MDD subtypes is urgently needed, to ensure the validity, generalisability, and clinical applicability of the subtypes identified. Therefore the current study aimed to identify latent MDD subtypes that connect diversified clinical manifestations and neural activities by utilising three methodologically rigorous approaches. First, we attempted to unveil distinct MDD subtypes based on the DSM-5 depressive symptoms by using latent profile analysis (LPA), which is a person-centred approach that pays attention to the heterogeneity of individual response patterns and defines unique subgroups in a sample. We then re-assessed symptom networks and neural activities between the identified MDD subtypes to verify the validity and the actual existence of these identified MDD subtypes. Network analysis was used to explore differences in symptom structures between these identified subtypes. The distinction of neural activity profiles between these identified MDD subtypes was also tested by using resting-state functional neuroimaging data. Both regional autonomic neural activity and functional connectivity networks were examined. Finally, the associations between symptoms of identified MDD subtypes and specific neural activity alterations were established. Moreover, the reproducibility of the classification was validated in an independent dataset. We hypothesised that: a) MDD could be further classified into more than one subtype based on the selected depressive symptoms; b) the symptom structures of the identified MDD subtypes would be significantly different between subtypes; and c) statistically significant associations would be expected between brain function and specific MDD subtypes, and subtype-specific abnormalities in brain function would be linked to the dominant symptoms of certain subtypes.

Methods

Ethics

The study was approved by the Ethics Committee of the Second Xiangya Hospital of Central South University (reference no. 2017020). All study participants agreed to participate in the study and provided written informed consent.

Participants

This cross-sectional study included two datasets from two different Chinese MDD outpatient cohorts, namely a discovery dataset and a replication dataset.

Discovery dataset

The discovery dataset originates from a large Chinese longitudinal MDD outpatient cohort, including outpatients with MDD and demographically matched healthy controls (HC). All participants were Chinese and had detailed clinical and neuroimaging data.

A total of 270 patients with MDD were recruited at the baseline of the cohort from 2016 to 2022 from the psychological clinic at the Second Xiangya Hospital of Central South University, Changsha, China. The MDD diagnosis was established by two experienced psychiatrists using the Structured Clinical Interview for DSM-IV-TR Axis I (SCID-I). Individuals who meet DSM-IV criteria for (unipolar) major depressive disorder and seek treatment for a currently active, nonpsychotic major depressive episode were included. The exclusion criteria for patients were diagnosis of other axis I psychiatric disorders, a history of major medical or neurological problems, and the presence of psychotic symptoms during major depressive episode. The present study utilised data from its baseline data collection, which had complete information on demographic and clinical characteristics, as well as neuroimaging data (including resting-state functional and T1 structural MRI). Meanwhile, a total of 105 HC were simultaneously recruited from local colleges and communities in Changsha from 2017 to 2022. The exclusion

criteria for HC were a history of any psychiatric disorders and any major medical or neurological problems. Of note, HC were not used for LPA-based MDD subtype identification but were used to help identify differences in neural activity between identified subtypes. Specifically, in addition to direct pair-wise comparison of brain activity between the identified MDD subtypes, another approach was used to uncover the differences between MDD subtypes which indirectly identifies different neural activity patterns between MDD subtypes by comparing them to the same HC sample.[22,34] In this case, HC were treated as a reference group for all MDD subtypes, and the differences between MDD subtypes would be indirectly discovered when different MDD subtypes presented various patterns compared to same reference group.

To accurately verify the differences in brain function between identified MDD subtypes, participants who failed to complete the magnetic resonance acquisition or had poor fMRI data quality (e.g., participants who demonstrated a maximum displacement greater than 2-mm or more than 2° of angular rotation on functional neuroimage) were excluded (see more detail in MRI preprocessing). All participants included were right-handed as assessed by the Edinburgh Handedness Inventory (EHI)[35] to exclude participants who were left-handed since potential differences in brain structure and function exist based on handedness.[36] Finally, a total of 259 patients with MDD and 92 demographically matched HC were included in the discovery dataset after screening the above criteria, while the age range at inclusion for MDD was 16–48 years, and 18–36 years for HC.

Replication dataset

The replication dataset comes from another Chinese cross-sectional MDD outpatient cohort with detailed clinical data but without neuroimaging data. A total of 92 patients with MDD were recruited from 2016 to 2024 from psychological clinic, also from the Second Xiangya Hospital of Central South University. The inclusion and exclusion criteria were the same as the discovery dataset. To ensure comparability between MDD patients in discovery and replication datasets, the patients with MDD in the replication dataset were matched with those patients in discovery dataset on demographic characteristics. Finally, a total of 86 patients with MDD were included in the replication dataset, to test the reproducibility of classification observed in the discovery dataset (see Classification testing in an independent replication dataset for details). The age range at inclusion was 16–44 years.

Measurements

Sociodemographic and clinical characteristics were collected. Depressive symptoms were assessed by the Beck Depression Inventory (BDI) and Hamilton Depression Rating Scale-17 items (HAMD-17). The medication status (yes or no) of patients was confirmed by clinical interviews and medical records, and defined according to previous studies as "not taking medication for at least 4 weeks", to serve as a "wash-out" state,[37–39] referring to a medication-free period long enough to allow the medication's effects to subside and minimise its potential influence on brain function. In the current study, "yes" means they were using antidepressants or antipsychotic medications when enrolled, and "no" means that the patients were medication-naïve, or they had washed off medications for at least 4 weeks prior to the day when they were enrolled.[38] The details of the medication status (including medication types, duration of medication, and dosage) for each patient with MDD are presented in Supplemental spreadsheet. Intelligence was assessed by the age-adjusted scores of subtests (information, similarity, arithmetic, and digit span) of the Chinese version of the Wechsler Adult Intelligence Scale-Revised (WAIS-RC)[40] to control participants' intelligence levels (WAIS-RC was not assessed in the replication dataset).

To identify MDD subtypes, ten symptoms were extracted and recoded from the BDI and HAMD-17 reflecting the nine depressive symptoms in the DSM-5 definition and an additional "feeling anxious" symptom. The reasons for including the "feeling anxious" symptom were: (1) as the DSM-5 declared, anxious distress has been noted as a prominent feature of both bipolar and major depressive disorder in both primary care and speciality mental health settings with highly prevalence[41]; (2) previous studies have demonstrated that anxiety symptoms can influence neurobiological and treatment response patterns within MDD[42]; and (3) other MDD subtyping studies also revealed that anxiety symptoms demonstrate a high degree of discriminative capacity in parsing the heterogeneity of MDD.[11,22,43] Thus, incorporating anxiety symptoms helps capture overlapping and distinct symptom profiles, enhancing the granularity of subtypes. All symptoms were extracted from BDI and HAMD-17 (Suppl. eTable S1 provides the item sources and their scoring ranges). The scores of all symptoms were recoded based on the item scores that constituted each symptom because some symptoms were measured by a single item, whereas others were assessed through combination of multiple items. For symptoms measured by a single item, the symptom score remains unchanged. For symptoms consisting of multiple items, the maximum value on any one of these items was used as the symptom score to represent the individual's severity of the symptom (since different items jointly reflect the same symptom dimension). Thus, a total of ten symptoms (*depressed mood, loss of pleasure, worthlessness/guilt, suicidal ideation, weight/appetite loss, sleep reduction, psychomotor symptom, fatigue/loss of energy, indecisiveness, and feeling anxious*) were used for subsequent analyses. The range of scores for *psychomotor* and *feeling anxious* are 0–4, and range of other symptoms are 0–3.

MRI acquisition and processing

MRI acquisition

The MRI was conducted on a Siemens Skyra 3.0T magnetic resonance scanner at the Second Xiangya Hospital of the Central South University. Subjects were asked to lie on the scanner, foam pads were used to fix their head to minimise head motion. The scanning sessions and the parameters were as follows: (1) three-dimensional T1-weighted, magnetisation-prepared rapid gradient echo (MPRAGE) sagittal images: repetition time (TR) = 1900 ms; echo time (TE) = 2.01 ms; slices = 176; slice thickness = 1 mm; voxel size = 1.0 × 1.0 × 1.0 mm; flip angle = 9°; inversion time = 900 ms; field of view (FOV) = 256 mm; matrix = 256 × 256. (2) resting-state fMRI series using the echoplanar imaging sequence: TR = 2500 ms; TE = 25 ms; axial slices = 39; slice thickness/gap = 3.5/0 mm; voxel size = 3.8 × 3.8 × 3.5 mm, 200 volumes; flip angle = 90°; FOV = 240 mm; matrix = 64 × 64. During the scanning, participants were instructed to keep their eyes closed but remain awake.

MRI preprocessing

MRI data preprocessing were performed using the Data Processing & Analysis for Brain Imaging (DPABI version 5.2, https://rfmri.org/DPABI/)[44] in Matlab R2013b. The preprocessing procedures were as follows: (1) raw DICOM data were converted to NIfTI format; (2) the first ten volumes were discarded to allow the magnetisation to reach equilibrium and for the participants to adapt to the scanning noise; (3) slice-timing correction and realignment of head motion. Participants who demonstrated a maximum displacement greater than 2 mm or more than 2° of angular rotation were excluded from this study; (4) T1-weighted images of each participant were co-registered to the mean functional images; (5) linear detrending, regressing out of nuisance covariates (WM signal, CSF signal, and Friston-24 head motion parameters) were performed to remove low-frequency drift; (6) functional images were normalised to the standard Montreal Neurological Institute (MNI) space using the transformation (co-registered T1 to standard MNI) parameters and resampled to 3 × 3 × 3 mm.

After preprocessing, three local indicators, namely the amplitude of low-frequency fluctuation (ALFF), fractional ALFF (fALFF), and regional homogeneity (ReHo), were calculated to reflect regional autonomic neuronal activity. In addition, one global indicator, the functional connectivity network (FCN), was computed to capture the coordination and interaction of neural activity between anatomically distributed but functionally related brain regions. These measures were used for further statistical analyses.

ALFF, fALFF, and ReHo calculation

For local indicators, ALFF, fALFF, and ReHo were obtained to reflect spontaneous neural activity. For ALFF value, spatial smoothing with a 6 mm full-width half maximum (FWHM) Gaussian filter was performed after preprocessing to reduce spatial noise. Then, the filtered time series was transformed into the frequency domain with a fast Fourier transform (FFT), and the power spectrum was obtained. To obtain ALFF value, the power spectrum was square-rooted and averaged (mean) across 0.01–0.08 Hz at each voxel, the obtained square root was referred to as the ALFF.[45] In order to standardise ALFF value across participants, the ALFF of each voxel was divided by the global mean of ALFF values for each participant.[45] For fALFF, the sum of the amplitude values in the 0.01–0.08 Hz low-frequency power range was divided by the sum of the amplitudes over the entire detectable power spectrum (range: 0–0.25 Hz).[46] Then, the fALFF value of each voxel was then divided by the global mean fALFF value for each participant to reduce the global effects. For ReHo value, temporal bandpass filtering at 0.01–0.08 Hz was performed to reduce physiological low-frequency drift and high-frequency noise. Then, Kendall's Coefficient of Concordance (KCC) was applied to calculate the similarity between a single voxel and the surrounding 26 voxels,[47] producing a regional homogeneity (ReHo) map for each subject. Subsequently, mean ReHo transformation was performed for standardisation purposes, by dividing the KCC among each voxel by the averaged KCC of the whole brain. Finally, the data were smoothed with a 6 mm FWHM Gaussian kernel.

Functional connectivity network calculation

In addition to local indicators, FCN was also calculated. For FCN, spatial smoothing with a 6 mm FWHM Gaussian filter was performed after preprocessing to reduce spatial noise, and then temporal bandpass filtering at 0.01–0.08 Hz was performed to reduce physiological high-frequency noise. The frame-wise displacement (FD) by Jenkinson et al.[48] was calculated to take into account voxel-wise differences in motion in its derivation. According to recommendations,[49] a "scrubbing routine" was used to censor any frame with an FD > 0.2 mm from the following FCN calculation. After scrubbing, all including participants had at least 79.5% of frames that remained to be calculated, which satisfied the analysable requirements (60%) outlined in Power et al.[50] (see mean FD and % frames censored in Table 1). The mean FD was further controlled as a covariate in the group-level imaging statistical analysis. Schaefer multiresolution atlas (100 cortical regions)[51] and Xiao's structural connectomic atlas (22 subcortical structures)[52] were used to generate a whole-brain correlation matrix for each subject. Thus, we calculated 122 × 122-element correlation matrices for all participants and 7381 connections for each participant were obtained.

Characteristics	Discovery dataset		Replication dataset	Between MDD in two datasets		Discovery dataset MDD vs. HC	
	MDD (N = 259)	HC (N = 92)	MDD (N = 86)	t/χ^2	p	t/χ^2	p
Age (years)	22.78 (5.95)	22.29 (3.95)	21.84 (6.02)	1.275	0.203	0.887	0.376
Sex (male/female)	86/173	39/53	21/65	2.329	0.127	2.499	0.114
Intelligence score[a]	47.44 (8.53)	51.67 (6.84)	NA	NA	NA	−4.762	<0.001
Duration (month)	22.06 (28.05)	NA	26.67 (30.65)	−1.288	0.199	NA	NA
Age of onset	20.52 (5.95)	NA	19.22 (6.55)	1.713	0.088	NA	NA
Medication (yes/no)[b]	100/159	NA	32/54	0.054	0.817	NA	NA
HAMD	19.59 (5.94)	NA	19.98 (5.80)	−0.534	0.594	NA	NA
BDI	29.92 (9.12)	6.38 (6.03)	29.09 (10.75)	0.697	0.486	27.791	<0.001
FD	0.05 (0.02)	0.05 (0.03)	NA	NA	NA	−0.037	0.971
Frame censored (%)[c]	0.02 (0.04)	0.02 (0.03)	NA	NA	NA	0.310	0.757

Notes: Means with standard deviations in parentheses. t/χ^2: variables of age, intelligence score, BDI, HAMD, and FD were tested by two-sample t-test as indicated by t; variable of sex was tested by chi-square test. The significance was set as $p < 0.05$ (two-tailed, t-test or chi-square test). **Abbreviations:** MDD, major depressive disorder; HC, healthy controls; HAMD, Hamilton Depression Rating Scale; BDI, Beck Depression Inventory; FD, frame displacement; NA, not applicable; WAIS-RC, the Chinese version of the Wechsler Adult Intelligence Scale-Revised. [a]Intelligence score: age adjusted scores of subtests of the short form of the WAIS-RC (including Information, Similarity, Arithmetic, and Digit span), which is only used for controlling the participants' intelligence level, rather than an estimation of intelligence quotient. [b]Medication: number of patients taking medicine yes/no. "No" means that the patients were medication-naïve, or they did not take any antidepressant or antipsychotic medication at least for 4 weeks prior to the day when they were enrolled in the study. "Yes" means they were using at least one medication when enrolled (including selective serotonin reuptake inhibitors, serotonin and norepinephrine reuptake inhibitors, tricyclic antidepressants, and atypical antidepressants and/or antipsychotics). [c]Frame censored (%): percentage of frames that were excluded from the further analysis after "scrubbing routine", which is a method used to remove unreliable data point due to excessive head motion (FD > 0.2 mm) in the functional neuroimaging data.

Table 1: **Demographic, clinical, and fMRI measures between two datasets and between MDD and HC in Discovery dataset.**

Statistics

Demographic and clinical characteristics were compared using chi-square tests and two-sample t-tests: between patients with MDD across the two datasets and between patients with MDD and HC in the discovery dataset. The significant p-value was set to 0.05 (two-tailed). There was no structured missingness in the current data (Suppl. eMethod S1), and the missingness of all the studied variables was less than 5%. The group mean values of continuous variables were used for imputation. There were no missing values for the categorical variables (e.g., sex and medication status). These statistical analyses were conducted with SPSS 29.0 software. Fig. 1 illustrates the overall analytical procedures for the present study, starting with the identification of MDD subtypes in the discovery dataset, followed by the validity verification of identified subtypes from both the symptom structure and neural activity perspectives, and ending with the testing of the reproducibility of the classification in the replication dataset.

Identification of MDD subtypes

LPA was used to characterise MDD subtypes based on heterogeneous clinical symptoms. LPA is a person-centred approach that pays attention to the heterogeneity of individual response patterns and defines unique subgroups in a sample.[53] LPA has fewer prerequisites for application, more reasonable clustering criteria and result testing, and less arbitrariness than traditional clustering methods (e.g., k-means),[54] which makes LPA particularly well-suited for exploring the latent structure of symptom profiles in psychiatric research (Suppl. eMethod S2).

LPA requires different estimation methods for data with different distributions. If the data satisfies normal distribution, the maximum likelihood (ML) should be used; but if the variables are skewed or non-normally distributed, more robust estimators were more appropriate for robust estimation (e.g., ML with robust standard error (MLR)).[55,56] We tested LPA models by using the MLR method due to the non-normal distributions of the 10 symptoms being investigated. The number of clusters was determined by the model fit statistics and interpretability.[57] According to the guidelines for fit indices, Akaike's information criteria (AIC), Bayesian information criteria (BIC), and sample-size adjusted BIC (aBIC) were used, with a lower value indicating superior fit. Lo–Mendell–Rubin (LMR) tests and bootstrapped likelihood ratio tests (BLRTs) were also conducted to evaluate the significance of model improvement between k-profile solution and k-1 profile solution. In addition, the relative *entropy* value was reported to evaluate the classification accuracy, with the *entropy* value greater than 0.8 indicating an acceptable model fit, and greater than 0.9 indicating a good model fit. Models with one to six clusters were tested. Moreover, we took "depression severity" (BDI total score) and "illness duration" as covariates when performing LPA. Some previous symptom-based classifications have identified different subtypes that differ primarily in symptom severity,[8,43,58] however, the current study assumes that different depression subtypes differ in

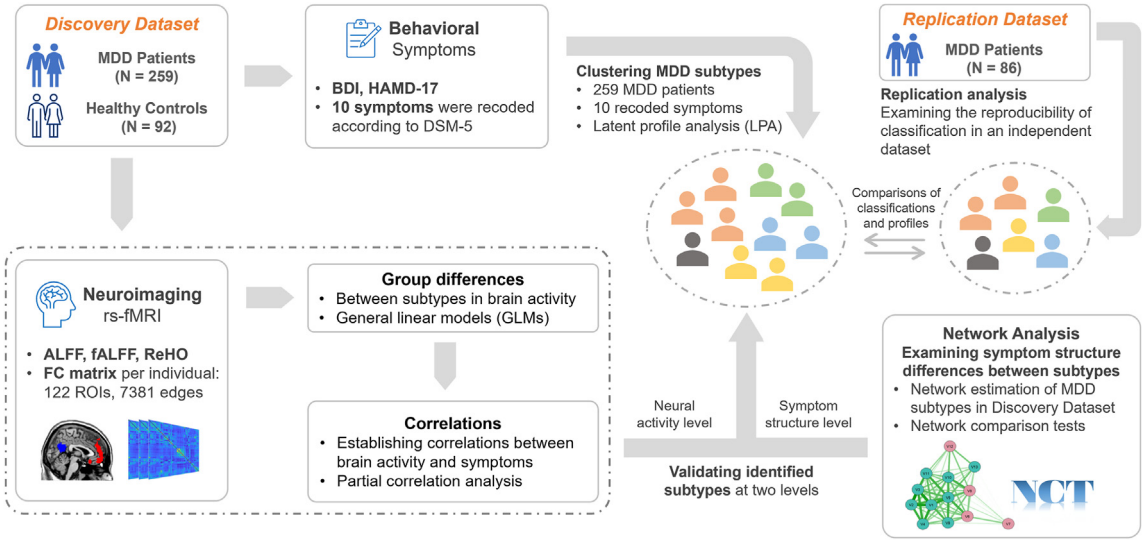

Fig. 1:* A schematic diagram of the analytical procedures in the current study.** The analytical procedures start with the identification of MDD subtypes in the discovery dataset, followed by the validity verification of identified subtypes at both the symptom structure and neural activity levels, and ending with the classification reproducibility test in the replication dataset. The sample sizes of patients with MDD and healthy controls in the discovery dataset are 259 and 92, respectively. The sample size of patients with MDD in the replication dataset is 86. ***Abbreviations: MDD, major depressive disorders; rs-fMRI, resting-state functional magnetic resonance imaging; BDI, Beck depression inventory; HAMD-17, Hamilton depression rating scale-17 items; DSM-5, Diagnostic and Statistical Manual of Mental Disorders: fifth edition; ALFF, amplitude of low-frequency fluctuation; fALFF, fractional ALFF; ReHo, regional homogeneity; FC, functional connectivity; ROIs, regions of interest.

clinical symptom manifestation patterns, with the aim of identifying depression subtypes with different symptom structures. Therefore, the overall severity of depressive symptoms was controlled for and we do not expect to obtain different classification results simply due to different symptom severity. At the same time, since the chronicity of depression (longer illness duration) is linked to more severe depressive symptoms and manifests as symptoms which are difficult to relieve,[59] "illness duration" was also controlled. Overall, by controlling "depression severity" and "illness duration", we ensure that differences between subtypes reflect inherent distinctions in symptom profile rather than the progressive changes associated with severity and chronicity. A total of 259 patients with MDD in the discovery dataset were included in the LPA model. All analyses were performed in Mplus version 8.3. Once the MDD subtypes were identified, two sets of verification tests (network analysis and fMRI analysis) were then conducted to validate the existence of the identified MDD subtypes.

Comparisons of symptom patterns across the identified MDD subtypes

To explore whether the identified MDD subtypes differed clinically in their symptom structures, the network estimation and network comparison tests were performed. Network analysis is a computational method, which is used to assess symptom-symptom interactions and identify 'central' symptoms of the network.[60] Network analysis was performed in R version 4.3.1.

Network estimation and centrality. The graphical Least Absolute Shrinkage and Selection Operator (glasso) was employed to estimate network structure of ten symptoms in patients with MDD by using the "bootnet" R package (version 1.5.3),[61] which could control for false positive edges with very small edges shrinking to zero. Edges with an edge weight (strength of connection) of 0 are not included in the network, suggesting that the relevant nodes are independent after controlling for all other relationships within the network. A network includes nodes (symptoms) and edges (connections between symptoms). Thicker and more saturated edges indicate stronger correlation between nodes.

The network structure was quantified by network centrality using "qgraph" R package (version 1.9.5).[62] Two centrality indices, node strength and expected influence, were estimated. Node strength to reflect the sum of all associations of a given node with all other nodes, which is a common and stable central metric,[63] while expected influence is the sum of the edge weights, accounting for the edges' signs, which is more sensitive when a node has both positive and negative edges. The accuracy of edge weights was tested using

"bootnet" R package (version 1.5.3),[61] using non-parametric bootstrapping (1000 bootstrap samples) to estimate the 95% confidence intervals (CIs), with the narrower the CIs, the higher the accuracy of edge weights. The correlation stability coefficient (CS-coefficient) was also estimated to assess the stability of the order of edge weights and strength centrality, with a total of 1000 bootstrapped samples used. The CS coefficient discerns the maximum proportion of participants that can be omitted from the analysis while still obtaining results with a strong correlation ($r > 0.70$) compared to the original findings, which a CS coefficient of >0.25 indicating adequate stability and preferably above 0.50.[61]

Network comparison test. To test whether symptom connectivity differs between MDD subgroups, network comparison tests (NCTs) were carried out using the "NetworkComparisonTest" R package (version 2.2.1).[64] Permutation tests with 1000 permutations were adopted to compare the networks of different subgroups on invariance of global network structure, global strength (overall level of connectivity of a network), and individual edge strength (post-hoc test if significant differences in global network structure were found). A resulting p value < 0.05 (network comparison test) indicates a significant difference.

Comparison of neural activity across the identified MDD subtypes

To explore whether the identified MDD subtypes differed in neural activity, analyses of covariance (ANCOVAs) within a general linear model (GLM) framework were used to test the differences in both local (ALFF, fALFF, and ReHo, conducted with Statistical Parametric Mapping 12 toolbox, SPM12, https://www.fil.ion.ucl.ac.uk/spm/software/spm12/) and global (FCN using Network-based statistic toolbox, NBS, version 1.2, https://www.nitrc.org/projects/nbs/) brain function indicators in Matlab R2013b, with age, sex, intelligence, and mean frame-wise displacement were adjusted as covariates in all tests.

First, neural activity differences between the overall patients with MDD and HC were examined. To determine how each MDD subtype contributed to these differences between overall MDD and HC, post-hoc tests were performed on the signals and/or the values extracted from brain regions and FCs that showed significant differences in the overall MDD vs. HC comparison, thereby identifying both shared and subtype-unique neural activity abnormalities. False discovery rate (FDR) correction was adopted for post-hoc tests in Matlab R2013b and all p-values from these tests were adjusted by considering both the number of comparisons (5 MDD subtypes vs. HC) and the total number of neural activity indicators, with a significance threshold of $pFDR < 0.05$.

Then, two different approaches were used for testing neural activity features that differed between identified MDD subtypes: one was a direct pairwise comparison of brain activity between the identified MDD subtypes, and another was an approach as has been done in previous studies[22,34] to uncover the differences between MDD subtypes, which indirectly identifies different neural activity patterns between MDD subtypes by comparing them to the same HC. The differences between MDD subtypes would be indirectly discovered when different MDD subtypes presented various patterns compared to the same HC. For both local and global indicators, one-tailed tests were applied to examine the differences between groups in both directions by defining comparison contrasts (e.g., Group 1 < Group 2, and/or Group 1 > Group 2) in SPM12 and NBS version 1.2, specifically testing whether the indicators were either increased or decreased in MDD compared to HC, as well as in comparisons between MDD subtypes.

For local indicators, ALFF, fALFF, and ReHo maps were enhanced by the probabilistic threshold-free cluster enhancement (pTFCE) method[65] to increase the detectability of neuroimaging signal, and image comparisons were corrected for multiple comparisons at the whole-brain level using family-wise error (FWE) correction to reduce potential false positives, with a significant threshold of cluster-level $p < 0.05$, starting from an uncorrected $p < 0.001$ at the voxel level. As suggested by Spisák et al.,[65] this method is robust to the cluster topology and provides a strict control over false positives, balancing the sensitivity and robustness. For the global indicator-FCN, permutation tests with 10,000 permutations and FDR correction were adopted for multiple comparisons corrections with the significance threshold set at 0.05 to reduce false positives due to a large number of FCs (7381 edges) (Suppl. eMethod S3 provides the rationale of utilising different multiple comparison correction methods for local and global indicators and their respective advantages). Moreover, since a total of ten comparisons were made when directly comparing between subtypes, Bonferroni correction was further adopted to correct the p values of the group differences between subtypes, with the significance threshold of $pFWE$ *or* $pFDR < 0.005$ (0.05/10 comparisons). In the indirect comparisons of different subtypes with the same HC, a total of five comparisons were made, and Bonferroni correction (with a threshold of $pFWE$ *or* $pFDR < 0.01$) was also performed (0.05/5 comparisons).

Association between neural activity and depressive symptoms

To further explore specific associations between functional alterations and depressive symptoms, the signals of brain regions in local indicators and the strengths of FCs that exhibited significant differences between MDD subtypes were extracted for subsequent partial correlation analyses with symptoms, controlling for age, sex, and intelligence score. Given the multiple comparisons involved in the partial correlation analyses, the p-values

were corrected using FDR, with the significance threshold of FDR $q < 0.05$. Partial correlation analyses were performed in SPSS 29.0, followed by FDR correction of p values in Matlab R2013b.

Sensitivity analysis

To test whether taking the medication would influence our MDD classification and their neural activities, we conducted the following sensitivity analyses: 1) The status of medication use was controlled during the LPA modelling process, to test whether the classification of MDD would be changed; 2) We divided the MDD group into MDD medicated and MDD unmedicated groups and tested if these two groups were comparable in terms of their sociodemographic characteristics using two-sample t-test and chi-square test, with the significant p-value of 0.05 (two-tailed). We then conducted LPA models separately for medicated and unmedicated groups to test the stability of identified MDD subtypes in the medicated and unmedicated groups; 3) We tested whether there were significant differences between MDD medicated and MDD unmediated groups in neural activity by using ANCOVA within a framework of GLM, with age, sex, intelligence score, and frame displacement as covariates, to clarify whether the differences in neural activity between the identified subtypes were influenced by medication status. FDR correction was applied for multiple comparisons, as multiple indicators were compared simultaneously. Significance was set as $pFDR < 0.05$.

Classification testing in an independent replication dataset

To further test the generalisability of the MDD subtypes classification, the same LPA procedures as in the discovery dataset were performed in the replication dataset (n = 86) to determine whether the number and characteristics of subtypes identified in the discovery dataset could also be observed in the replication dataset.

Role of funders

The funders had no role in study design, data collection, data analyses, interpretation, or writing of reports.

Results

Identification of latent MDD subtypes

Table 1 summarises demographic and clinical characteristics of all participants, and Suppl. eTable S2 provides demographic and clinical characteristics for males and females separately. In the discovery dataset, 259 patients with MDD (66.8% females) and 92 demographically matched HC (57.6% females) were included. There were no significant differences between patients with MDD and HC in age (two-tailed $p = 0.376$, two-sample t-test) and sex ration (two-tailed $p = 0.114$, chi-square test), while a significant difference was found between them in the intelligence score (two-tailed $p < 0.001$, two-sample t-test). Patients with MDD showed significantly higher scores in BDI compared to HC (two-tailed $p < 0.001$, two-sample t-test). In addition, no significant differences were observed in FD and proportion of frame censored between patients with MDD and HC (two-tailed $p > 0.05$, two-sample t-tests).

A total of 259 Chinese patients with MDD in the discovery dataset were included to characterise the subtypes based on the DSM-5 depressive symptoms by utilising the LPA model. After considering the model fit and interpretability, the optimal 5-class solution of the LPA model was selected to characterise MDD subtypes (AIC = 6656.296, aBIC = 6681.030, entropy = 0.917, LMR $p = 0.3267$ [Lo–Mendell–Rubin test], BLRT $p < 0.001$ [bootstrapped likelihood ratio test]) (Suppl. eTable S3 provides the fit indices for each solution of LPA). Suppl. eTable S4 presents the mean posterior probabilities for patients in each class, and the results showed that the average probability of each class of patients belonging to their respective class was more than 90%, indicating a high accuracy of classification. The final LPA-derived classification revealed five clinical distinct MDD subtypes with differential prevalence patterns: class 2 comprised the largest proportion (38.6%, n = 100), followed by class 5 (19.3%, n = 50). Classes 1 and 4 each accounted for 15.4% of the total sample of the patients with MDD (n = 40 for class 1 and n = 40 for class 4), while class 3 constituted the smallest subtype (11.2%, n = 29). Demographic and clinical features of each identified subtype are presented in Suppl. eTable S5.

Fig. 2 illustrates the symptom profiles of the five identified MDD subtypes. As shown in Fig. 2, class 1 exhibited the lowest severity of all the symptoms studied, especially symptoms that reflect melancholic features (e.g., *weight/appetite loss, sleep reduction*). The dominant symptoms of patients in this group were *depressed mood, worthlessness/guilt, fatigue/loss of energy*, accompanied by *feeling anxious* (Suppl. eTable S6 provides the ranked dominant symptoms of each identified subtype). Although we were unable to measure atypical features (for instance, increased weight/appetite, hypersomnia) directly, the present characteristics as well as evidence of abnormal brain activities (see Differences in brain function between MDD subtypes for details) suggested that this group may represent some atypical-like features among these patients with MDD. Therefore, we labelled class 1 as "atypical-like depression, AD" (n = 40).

Class 2 captured those with relatively higher scores on melancholic features, but a lower score on *loss of pleasure*. This class was defined as "moderate melancholic depression, mMD" (n = 100).

Class 3 had a higher score on *loss of pleasure*, which was the most discriminating symptom compared to the other groups. Meanwhile, patients in this class also showed higher scores on *depressed mood, worthlessness/guilt, sleep reduction*, and *indecisiveness*. This class was

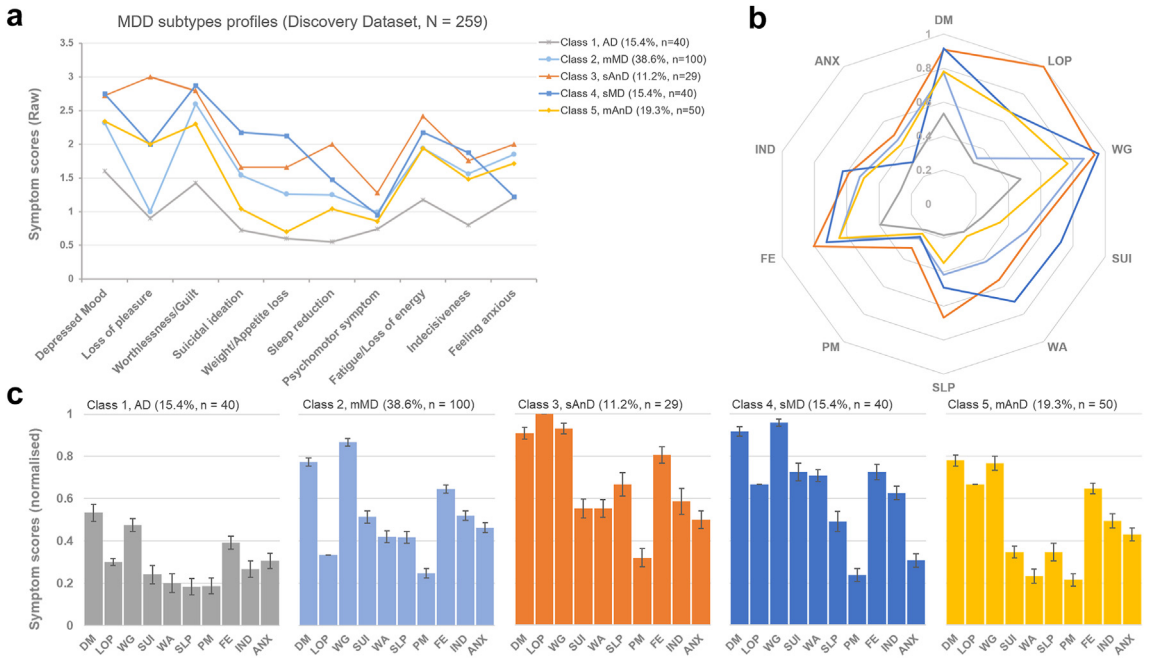

Fig. 2: **Symptom profiles of the identified five subtypes of major depressive disorder.** The sample sizes of five identified subtypes are: atypical-like depression (AD, n = 40); moderate melancholic depression (mMD, n = 100); severe anhedonic depression (sAnD, n = 29); severe melancholic depression (sMD, n = 40); moderate anhedonic depression (mAnD, n = 50). a) Five MDD subtypes identified based on the raw scores of considered symptoms in the latent profile analyses; b) Radar plot showing symptom patterns of identified subtypes using normalised scores, where values range from 0 to 1, representing the relative severity of each symptom; c) Bar charts using normalised symptom scores, with error bars representing 95% confidence intervals. ***Abbreviations:*** MDD, major depressive disorder; DM, depressed mood; LOP, loss of pleasure; WG, worthlessness/guilt; SUI, suicidal ideation; WA, weight/appetite loss; SLP, sleep reduction; PM, psychomotor symptom; FE, fatigue/loss of energy; IND, indecisiveness; ANX, feeling anxious.

therefore defined as "Severe anhedonic depression, sAnD" (n = 29).

Class 4 showed higher scores on those symptoms that were associated with melancholic features and showed a lower score on *loss of pleasure*. Another distinct feature is that patients in this group were more likely to report lower scores on *feeling anxious*. We named this class as "Severe melancholic depression, sMD" (n = 40).

Class 5 demonstrated moderate scores on *depressed mood*, *worthlessness/guilt*, *loss of pleasure*, *fatigue/loss of energy*. Patients in this class also reported *sleep reduction* but no obvious *weight/appetite loss*. This class was entitled as "moderate anhedonic depression, mAnD" (n = 50). Notably, although both mMD and sMD had melancholic features, they differed significantly on the symptom of *feeling anxious*. Similarly, although the dominant symptom in both mAnD and sAnD was *loss of pleasure*, they were significantly different on the symptom of *weight/appetite loss*. These distinctions were identified by the LPA processing as well as supported by their clinical manifestations, therefore they were classified as different subtypes.

Furthermore, the results of sensitivity analysis showed that the status of medication use did not change the result of MDD subtyping (Suppl. eTable S7 provides the results of group comparison between medicated and unmedicated groups in demographic and clinical characteristics and revealed no significant differences, Suppl. eResults S1 presents the detailed results of sensitivity analysis, Suppl. eFigure S1 provides profiles of MDD subtypes after adjusting medication status, and Suppl. eFigure S2 provides profiles of MDD subtypes observed in medicated and unmedicated groups separately).

Symptom networks of the identified MDD subtypes

Network structure, network accuracy, and network stability estimation results of the overall patients with MDD were presented in Suppl. eFigures S3–S5, respectively, revealing that 38 (84.4%) of all the possible 45 edges were estimated to be non-zero. The strongest edge was between "*worthlessness/guilt*" and "*suicidal ideation*". Besides, the network revealed strong associations between *depressed mood* with *worthlessness/guilt* and *loss of pleasure*. A strong association between *loss of pleasure* and *fatigue/loss of energy* was also found. *Psychomotor (agitation and retardation)* was weakly correlated with other symptoms. The symptoms with the

greatest strength centrality were *worthlessness/guilt*, *fatigue/loss of energy*, *depressed mood*, and *loss of pleasure* (Suppl. eFigure S3b illustrates strength centrality and expected influence for depressive symptoms). The correlation stability (CS) coefficient for node strength (CS = 0.44) and expected influence (CS = 0.517) centralities exhibited an acceptable and good level of stability, respectively.

To test whether the identified MDD subtypes had distinct symptom structures, network comparison tests were conducted. In the current study, since there were some symptoms with no variance (only 1 level) in each subtype, we then combined subgroups to compare them indirectly. As we found four symptoms with the greatest importance (determined by node strength and expected influence, Suppl. eFigure S1b), including "*worthlessness/guilt*", "*fatigue/loss of energy*", "*depressed mood*", and "*loss of pleasure*" in the network of overall MDD patients, we then ranked the dominant symptoms of each subgroup to identify groups with similar order of symptom domination across these four central symptoms. Normalised scores for each symptom were used to rank the dominant symptoms within each identified subtype. Since eight out of ten symptoms had a score range of 0–3 and the remaining two ranged from 0 to 4, we normalised all symptom scores to ensure comparability. The normalised scores were then ranked by severity to identify the relative dominance of symptoms within each subtype. Suppl. eTable S6 provides the ranked dominant symptoms of each identified subtype. Thus, mMD and sMD were combined accordingly since they showed similar order of symptom domination and the resulting subtype was named as "combined-melancholic depression, cMD" for further verification analysis. The CS-coefficient for node strength of cMD was 0.364. The cMD was set as baseline network, then we added other MDD subgroups into this combined group and tested if the network structure changed. If the network structure significantly changes after adding a subgroup, it suggests this added subgroup has a different network structure with cMD. The results of this method could provide indirect evidence on whether there were differences in the network structures of the added subgroup and the combined group. Specifically, we first added group AD, mAnD, sAnD into cMD, respectively and performed network comparison tests to examine whether there were significant differences between cMD with cMD + AD, cMD + sAnD, and cMD + mAnD, respectively. In order to test whether there were significant differences among AD, sAnD, and mAnD, we first compared the network of cMD + AD and cMD + sAnD to test the differences between AD and sAnD; then the network comparison test between cMD + AD and cMD + mAnD was also performed to test the differences between AD and mAnD; Finally, to reduce sources of heterogeneity, we compared networks between AD + sAnD and AD + mAnD to test whether there was significant difference between group sAnD and group mAnD. These results showed that cMD significantly differed from mAnD and sAnD in the symptom network structures (p = 0.017, p = 0.048, respectively, NCTs). The edge showing significant differences between cMD and both mAnD and sAnD was *loss of pleasure-weight/appetite*, (p < 0.001 for cMD vs. mAnD, and p = 0.035 for cMD vs. sAnD, NCTs with post-hoc tests). AD exhibited significant differences from mAnD and sAnD on network structures (p = 0.001, p = 0.010, respectively, NCTs). In addition, mAnD and sAnD showed significant differences on the global strength (p = 0.036, network comparison test) rather than the global network structure (p = 0.189, NCT). Suppl. eFigure S6 and Suppl. eResult S2 present the detailed results of network comparison tests.

Differences in brain function between MDD subtypes

Differences in local indicators

No significant differences between the overall MDD and HC groups were found in three local indicators. We compared each MDD subtype with HC and the results showed that some subtypes had unique brain functional alterations compared to HC (all $pFWE$ < 0.01, ANCOVAs based on GLM), whereas others did not (Table 2, Suppl. eFigure S7). These results indicate that the heterogeneity of MDD can be tested at the neuroimaging level and provide certain neurobiological evidence for these identified MDD subtypes. To further explore the differences in neuroimaging between subtypes, pairwise comparisons between subtypes were performed, and the results showed that sMD significantly differs from other four subtypes in terms of spontaneous neural activities (all $pFWE$ < 0.005, ANCOVAs based on GLM), while no significant differences were found between the other four subtypes. Table 2 presents the results of group comparisons based on these local indicators of brain function, and the Suppl. eFigure S7 presents the visualisation results of these brain regions that showed significant differences between groups.

Differences in functional connectivity networks

As shown in Fig. 3a, significant differences between the overall patients with MDD and HC in 17 FCs were observed (10,000 permutations and adjusted $pFDR$ < 0.05, ANCOVA based on GLM), especially in connections between the default mode network and subcortical regions. To further explore shared and subtype-unique neural activity abnormalities across MDD subtypes, post-hoc tests were performed, and the results suggested that AD, mMD, and sMD contributed most of the differences between overall MDD and HC within 17 FCs, they shared some FC alterations (Fig. 3b). For instance, compared to HC, these three subtypes shared FC alterations mainly involving in dorsal/ventral attention networks, default model

Brain region	Voxel	MNI coordinate			Peak T value	P_{FWE} (one-tailed)
		x	y	z		
Subtypes vs. HC						
ALFF						
sAnD > HC						
L. medial prefrontal cortex/anterior cingulate cortex (BA32)	165	−12	27	33	5.32	<0.001
sMD < HC						
L. inferior/middle temporal gyrus/temporal pole (BA20/36)	223	−33	6	−33	4.03	<0.001
R. inferior/middle temporal gyrus/ fusiform/temporal pole_(BA20/36)	491	42	0	−27	3.97	<0.001
fALFF						
sMD < HC						
B. praecuneus (BA7)	201	0	−63	45	4.61	<0.001
ReHo						
sMD > HC						
R. Precentral/postcentral gyrus (BA3/4)	40	39	−21	57	4.53	0.002
R. Superior temporal gyrus (BA22/48)	40	51	−6	3	3.69	0.002
Between subtypes						
ALFF						
mMD > sMD						
R. Temporal pole/parahippocampal gyrus (BA20/35)	208	42	3	−27	4.70	<0.001
sAnD > sMD						
R. medial prefrontal cortex (BA11/47/48)	875	12	42	30	4.74	<0.001
L. medial prefrontal cortex (BA11/47/48)	637	−3	48	15	4.56	<0.001
sMD < mAnD						
B. lateral prefrontal cortex/orbital frontal cortex (BA9/44/46/47/48)	1107	30	33	39	4.28	<0.001
B. orbital frontal cortex (BA11/24)	177	9	12	−27	3.85	<0.001
fALFF						
sMD < AD						
B. praecuneus (BA7)	116	0	−51	42	4.24	<0.001
ReHo						
mMD > sMD						
R. anterior cingulate cortex (BA11)	38	15	30	6	4.46	0.004

Notes: The significance level for these brain regions was set at $p < 0.05$, cluster-level family-wise error (FWE) corrected with voxel-level starting from $p < 0.001$ uncorrected after the probabilistic threshold-free cluster enhancement (ANCOVAs based on GLM); age, sex, intelligence score, and FD were taken as covariates. For the brain regions that are significantly different between subtypes, the significance was set at *pFWE* < 0.005 (Bonferroni corrected) due to a total of 10 comparisons being performed (ANCOVAs based on GLMs); for the brain regions that are significantly different between each subtype and HC, the significance was set at *pFWE* < 0.01 (Bonferroni corrected) due to a total of 5 comparisons being performed (ANCOVAs based on GLM). The notation *BA[number]* represents the specific location of a brain region within the Brodmann area (BA) system, with the number corresponding to a particular cortical area. ***Abbreviations:*** ALFF, amplitude of low-frequency fluctuation; fALFF, fractional ALFF; ReHo, regional homogeneity; FD, frame displacement; AD, atypical-like depression (n = 40); mMD, moderate melancholic depression (n = 100); sAnD, severe anhedonic depression (n = 29); sMD, severe melancholic depression (n = 40); mAnD, moderate anhedonic depression (n = 50); HC, healthy controls (n = 92); BA, Brodmann area; x, y, z, coordinates of peak locations in the Montreal Neurological Institute space (MNI); L, left hemisphere; R, right hemisphere; B, bilateral hemisphere; ANCOVAs, analyses of covariance; GLM, general linear model.

Table 2: **Group differences in local neural activity between MDD subtypes and between each subtype and healthy controls.**

network, and subcortical regions (all $pFDR < 0.05$, ANCOVAs with post-hoc tests). In addition, unique FC alterations were also observed in each subtype. While the two anhedonic depression subtypes were significantly different from HC in a small amount of these FCs (all $pFDR < 0.05$, ANCOVAs with post-hoc tests), especially in FCs involved in reward circuit (such as orbital frontal cortex and caudate). We also compared each subtype with HC in the whole-brain FCN, only AD showed decreased FCs compared to HC after strict multiple comparison corrections (Bonferroni correction with a threshold of $pFDR < 0.01$, ANCOVA based on GLM) (Suppl. eFigure S8 illustrates the differences in whole-brain FCN between AD and HC).

We further examined whether there were differences between subtypes in the whole-brain FCN by using pairwise comparisons. As shown in Fig. 3c, significant differences in certain FCs were observed across all pairwise subtype comparisons (all $pFDR < 0.005$, ANCOVAs based on GLM) except for comparisons between AD and sAnD, between mMD and mAnD, and between sMD and mAnD.

In addition, sensitivity analysis revealed no significant differences in neural activities between medicated and unmedicated patients with MDD in the brain regions/FCs where subtype differences were observed (all $pFDR > 0.05$, ANCOVAs based on GLM, medication effect on neural activities was presented in Suppl. eTable S8), indicating that taking or not taking an antidepressant or antipsychotic medication during the 4 weeks prior to study participation did not change the main findings observed in the current sample (Suppl. eResult S1 presents the detailed results of sensitivity analysis).

Correlations between brain activities and symptoms

Fig. 4 presents the partial correlations between brain activities and symptoms. The results indicated that most of the neural activities that differed between subtypes were significantly correlated with those symptoms that were different between subtypes (Suppl. eTable S9 provides the detailed coefficients of partial correlation analysis). In detail, sAnD and sMD differed in brain activities in regions involved in reward function (e.g., medial prefrontal cortex, insula, and globus pallidus), and brain activities in these regions were significantly correlated with *loss of pleasure* (all FDR $q < 0.05$, partial correlation analysis), which was the main difference in symptoms between sAnD and sMD. AD showed differences from other subtypes in FCs of insula-sensory cortex, and these FCs correlated with differential symptoms between AD and other subtypes (e.g., *loss of pleasure*, *weight/appetite loss*, *fatigue/loss of energy*, *indecisiveness*, etc.), with all correlations reaching significance after FDR corrections (all FDR $q < 0.05$, partial correlation analysis). Meanwhile, mMD and sMD showed differences in the ALFF value of the right parahippocampal gyrus/temporal pole, the ReHo value of right anterior cingulate cortex, and FCs of prefrontal cortex-substantia nigra, and these brain activities were significantly correlated with the certain symptoms (all FDR $q < 0.05$, partial correlation analysis) that differed between mMD

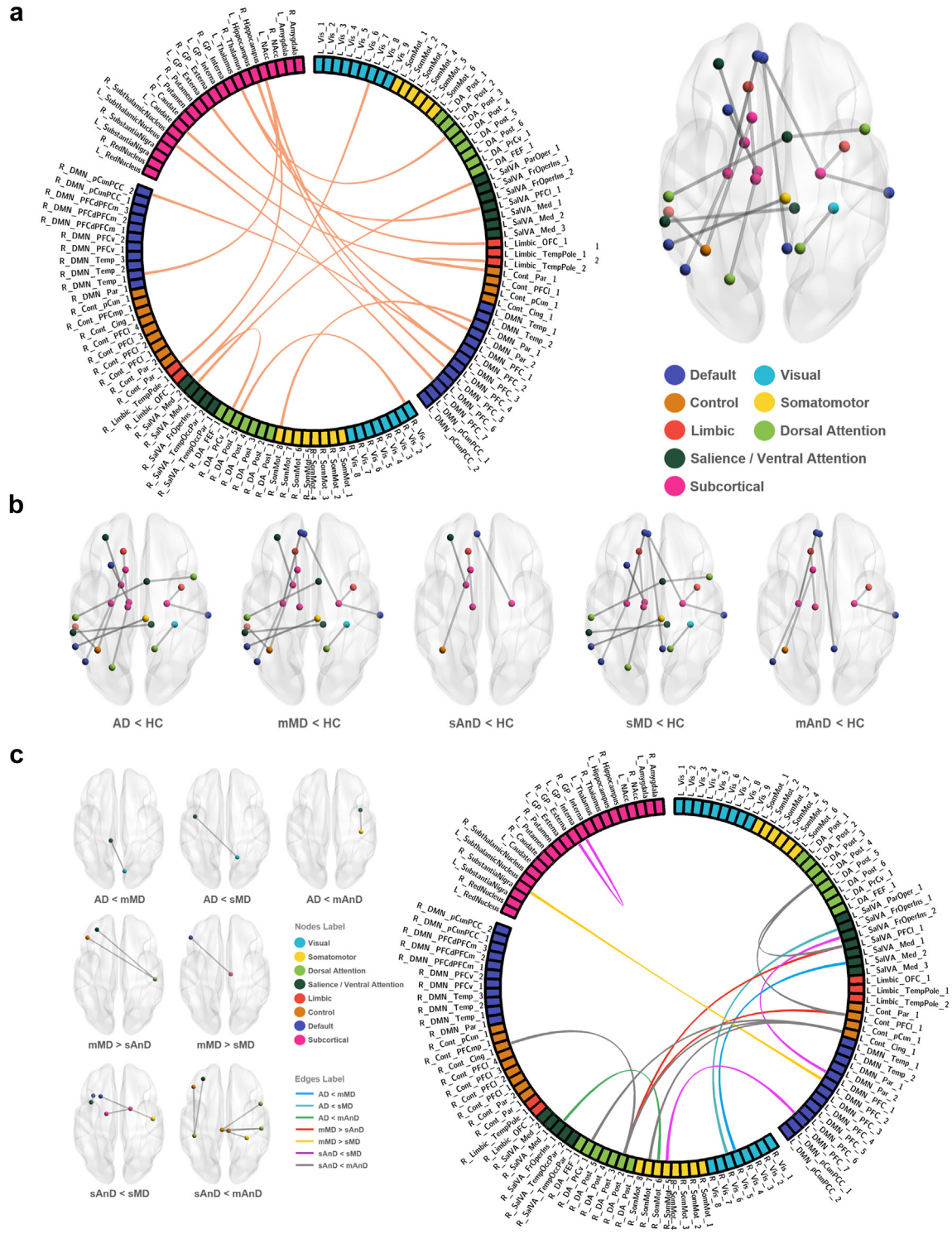

Fig. 3: **Group comparisons in functional connectivity network.** Circos plots and functional connectivity maps revealed significant differences a) between overall MDD (n = 259) and HC (n = 92) in whole-brain FCN (MDD < HC, *pFDR* < 0.05, ANCOVA based on GLM); b) between different MDD subtypes (AD, n = 40; mMD, n = 100; sAnD, n = 29; sMD, n = 40; mAnD, n = 50) and HC (n = 92) within 17 FCs that showed significant differences between overall MDD and HC (*pFDR* < 0.05, ANCOVA with post-hoc test); c) Results from pair-wise comparisons between the identified MDD subtypes (AD, n = 40; mMD, n = 100; sAnD, n = 29; sMD, n = 40; mAnD, n = 50), with the significance threshold of

and sMD (*loss of pleasure*, *feeling anxious*, etc.). In addition, the differences in symptoms between mAnD and sAnD were mainly manifested in *loss of pleasure* and *weight/appetite loss*, and the differences in brain activities between mAnD and sAnD were significantly related to these symptoms (all FDR $q < 0.05$, partial correlation analysis).

Reproducibility of subtyping in the replication dataset

As shown in Table 1, in the replication dataset, a total of 86 patients with MDD were included (75.58% females), and the demographic characteristics and clinical features exhibited no statistical significance between patients with MDD in the discovery and replication datasets (all two-tailed $p > 0.05$, two-sample t-tests or chi-square tests), suggesting that the groups of patients with MDD were comparable. The same LPA procedures as in the discovery dataset were performed in the replication dataset and the results also suggested that the 5-class solution should be selected as the optimal classification solution to characterise MDD subtypes in the replication dataset (AIC = 1952.744, aBIC = 1907.898, entropy = 0.933, LMR $p = 0.6464$ [Lo–Mendell–Rubin test], BLRT $p = 0.03$ [bootstrapped likelihood ratio test]) after considering the model fit and interpretability. Suppl. eTable S3 provides the fit indices for each solution of LPA. Suppl. eTable S4 also presents the mean posterior probabilities for patients in each class that were identified in the replication dataset. Similar to the discovery dataset, the average probability of each class of patients belonging to their respective class was more than 90%, indicating a high accuracy of classification. Meanwhile, like the LPA result in the discovery dataset, five identified MDD subgroups in the replication dataset exhibited similar latent symptom structures to those subtypes identified in the discovery dataset (Suppl. eFigure S9 illustrates the symptom profiles of the five identified MDD subgroups in the replication dataset and Suppl. eResult S3 provides detailed descriptions regarding each subgroup).

Discussion

The present study utilised a data-driven approach to explore clinical subtypes of MDD in real-world settings without presupposing how symptoms would cluster, presenting the MDD subtyping results based on both clinical features and neural activities, and neural correlations of clinical symptoms supported the coherence of these findings. Taken together, the functional neuroimaging discoveries and distinct patterns of symptom networks characterising MDD through different lenses and perspectives and the coherence of these findings further constellated the existence of these identified MDD subtypes. The replication analysis in an independent dataset verified the reproducibility of the identified MDD subtypes. Fig. 5 presents a summary of the main findings of the current study. The findings of the present study could have transformative potential in clinical decision-making and personalised management.

We included standard depressive symptoms of DSM-5 and identified five MDD subtypes. Unlike previous studies in which the characterisation of depression subtypes was based on symptom severity.[8–12] The five MDD subtypes in the current study showed different symptom patterns, including atypical-like depression (AD, n = 40, 16.3%), moderate melancholic depression (mMD, n = 100, 37.8%), severe melancholic depression (sMD, n = 15.7%), moderate anhedonic depression (mAnD, n = 50, 19.0%), and severe anhedonic depression (sAnD, n = 29, 11.2%). Consistently, *depressed mood*, *worthlessness/guilt*, as well as *fatigue/loss of energy* were dominant symptoms for most patients with MDD, which were stated in DSM-5.[41] Symptoms of *loss of pleasure* and *weight/appetite loss* were the most distinguishing symptoms among our identified subtypes. The present study identified 53.5% of MDD as melancholic depression (including moderate and severe melancholic depression) and 16.3% with atypical-like depression. These findings are consistent with previous studies that draw an overall picture of demographic and clinical features of Chinese patients with MDD. One study found that 53.4% of 1178 patients were classified as melancholic depression.[66] Another study discovered that the prevalence of atypical depression was 15.3%.[67] Meanwhile, for 30.2% of patients with MDD (50 patients in moderate anhedonic depression, 29 in severe anhedonic depression), their symptom patterns were dominated by *loss of pleasure* in the current study and were classified as anhedonic depression. As one of the core symptoms of MDD, anhedonic features are an important MDD phenotype. It is noted that, in severe melancholic depression subtype (15.7%), patients also showed obvious *loss of pleasure* symptoms, despite it not being the dominant symptom. Our findings were

pFDR < 0.005 after multiple comparisons corrections (ANCOVA based on GLM). In the Circos plots and functional connectivity maps, each node on the circumference or brain template represents a brain region, with different colours representing their corresponding brain networks, and the links between nodes indicating significant functional connectivity differences. Circos plots and functional connectivity maps were generated using Circos package (version 0.69-9) in Python 3.11 and BrainNet Viewer 1.7 in Matlab R2013b, respectively. ***Abbreviations:*** MDD, major depressive disorder; HC, healthy controls; AD, atypical-like depression; mMD, moderate melancholic depression; sAnD, severe anhedonic depression; sMD, severe melancholic depression; mAnD, moderate anhedonic depression; FCN, functional connectivity network; GLM, general linear model.

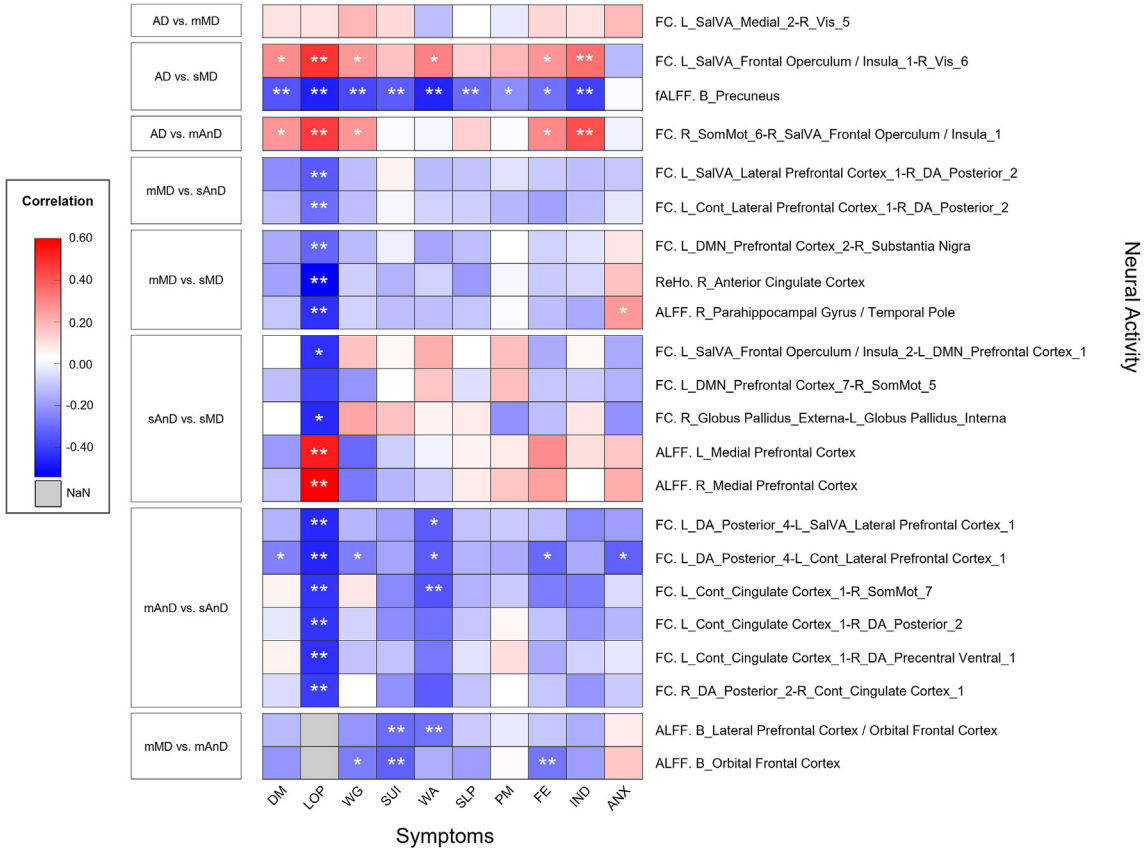

Fig. 4: **A heatmap illustrates correlations between neural activity indicators and symptoms.** Results from the partial correlation analysis, with age, sex, intelligence score, and FD included as covariates. The sample sizes of five identified subtypes are: atypical-like depression (AD, n = 40); moderate melancholic depression (mMD, n = 100); severe anhedonic depression (sAnD, n = 29); severe melancholic depression (sMD, n = 40); moderate anhedonic depression (mAnD, n = 50). The significance level was set as 0.05 after false discovery rate (FDR) correction. *FDR $q < 0.05$, **FDR $q < 0.01$ (Partial correlation analysis). Grey cells indicated missing values (NaN) due to the absence of variance in the corresponding symptom within this subgroup, making correlation analysis infeasible. The neural activity indicators presented on the right represent the spontaneous brain activity (ALFF, fALFF, and ReHo) in specific brain regions and the functional connectivity (FC) between different brain regions (nodes). For ALFF, fALFF, and ReHo, each feature is named as: *[Hemisphere]_[Region]*, in which *Region* corresponds to anatomical regions defined by the Automated Anatomical Labelling (AAL) template. Each FC is denoted using a hyphen between the two brain regions names (node labels). Cortical brain regions were defined using the Schaefer multiresolution atlas (100 cortical regions), where each region follows one of the two formats: *[Hemisphere]_[Network]_[Region]_[Index]*, or *[Hemisphere]_[Network]_[Index]*. Subcortical regions were defined based on Xiao's structural connectomic atlas (22 subcortical regions), following the format: *[Hemisphere]_[Region]*. Here, *Hemisphere* indicates the brain side, including left (L), right (R), or bilateral (B, if available), *Network* (cortical nodes only) refers to the functional network affiliation of that brain region (DMN, Default Mode Network; Cont, Control Network; SomMot, Somatomotor Network; DA, Dorsal Attention Network; SalVA, Salience/Ventral Attention Network; Vis, Visual Network), *Region* refers to the anatomical location, and *Index* denotes the parcel number within that network or region. The heatmap was generated in Matlab R2019b. ***Abbreviations:*** ALFF, amplitude of low-frequency fluctuation; fALFF, fractional ALFF; ReHo, regional homogeneity; FC, functional connectivity; FD, frame displacement; DM, depressed mood; LOP, loss of pleasure; WG, worthlessness/guilt; SUI, suicidal ideation; WA, weight/appetite loss; SLP, sleep reduction; PM, psychomotor symptom; FE, fatigue/loss of energy; IND, indecisiveness; ANX, feeling anxious.

consistent with a recent study that showed 51.97% of patients with MDD exhibited anhedonia symptoms with unique psychological and clinical features in a Chinese sample.[68] Moreover, the reproducibility of the characterisation in the current study was also verified in a replication dataset.

Furthermore, the validity of the current subtyping was supported by both symptom network structures and neural activity profiles. We found that melancholic depression differed from moderate anhedonic depression and severe anhedonic depression subtypes in network structures, primarily in the association between symptoms of *loss of pleasure* and *weight/appetite loss*. The neuroimaging findings also indicated the differences between melancholic and anhedonic subtypes as ALFF and FC involved in reward-related regions (mPFC,[69]

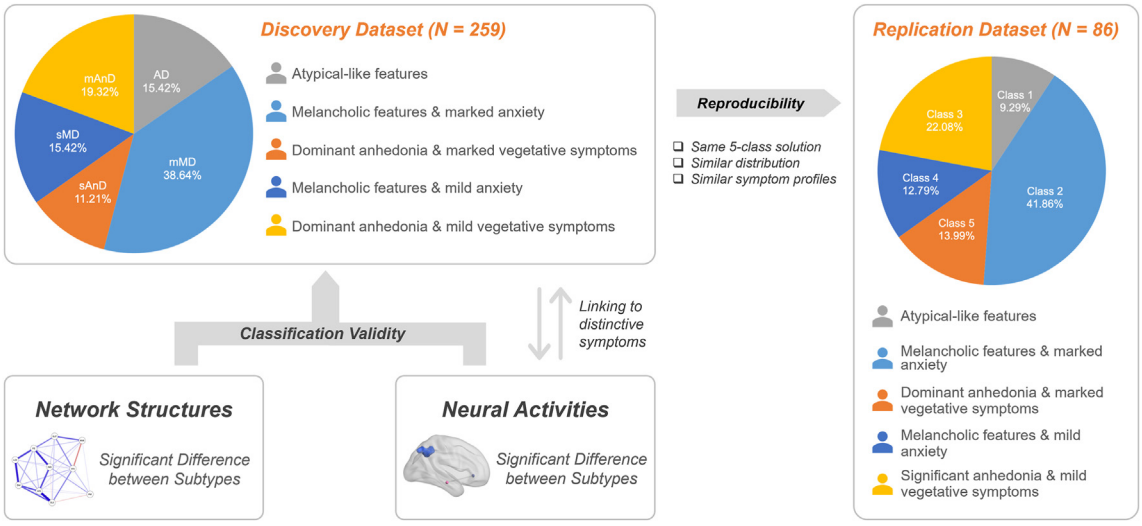

Fig. 5:* A summary of the main findings.** Five MDD subtypes were identified in the discovery dataset (N = 259) using latent profile analysis (LPA). Significant differences between identified MDD subtypes in both network structures and neural activities, along with neural correlations of clinical symptoms further support the validity of the classification. Replication analysis in the replication dataset (N = 86) confirmed the reproducibility of the classification, with the following sample sizes: class 1 (n = 8), class 2 (n = 34), class 3 (n = 19), class 4 (n = 11), and class 5 (n = 12). ***Abbreviations: AD, atypical-like depression (n = 40); mMD, moderate melancholic depression (n = 100); sAnD, severe anhedonic depression (n = 29); sMD, severe melancholic depression (n = 40); mAnD, moderate anhedonic depression (n = 50).

insula, and globus pallidus[70]). These correlation analyses supported the connection between the above-mentioned brain alterations and *loss of pleasure*. The symptom of *loss of pleasure* often encompasses multiple aspects, including reduced sensitivity to primary reward (e.g., food, sex) and secondary reward (e.g., money, entertainment).[71] Appetite loss is one of the critical dimensions of *loss of pleasure*.[70] However, they do not always appear together, as *appetite loss* can occur without having *loss of pleasure*, or vice versa.[70] For instance, both two melancholic subtypes showed significant *weight/appetite loss* but low levels of *loss of pleasure*; this was not the case for anhedonic subtypes. Low levels of *weight/appetite loss* were observed among the two anhedonic subtypes (especially in moderate anhedonic depression), although patients in these two subtypes reported relatively higher scores on the symptom of *loss of pleasure*.

It may be the case that *weight/appetite loss* symptoms manifested in different subtypes may have different underlying mechanisms. Correlation analyses suggested that *weight/appetite loss* and *loss of pleasure* in anhedonic depression were significantly correlated with reward-related FCs, with key nodes mainly including the middle cingulate cortex (MCC) and postcentral gyrus, suggesting that these two symptoms in patients with anhedonic depression may have a common neural basis. In other words, *weight/appetite loss* may be one dimension of *loss of pleasure* symptoms among patients of anhedonic subtype. Specifically, the MCC plays an important role in decision-making, especially in relation to reward.[72] The postcentral gyrus is the site of the primary somatosensory cortex with principal functions in proprioception and touch sensations and appears receptive to food stimuli.[73] Abnormal FC in these areas may be involved in abnormalities in the individual's anticipation and decision-making processing of reward cues (including food reward). Thus, reduced sensitivity to rewarding stimuli (delicious food) contributes to *weight/appetite loss* symptoms. These results are consistent with a recent review that concludes reward hyposensitivity is related to the anhedonic subtype of MDD being characterised by motivational deficits.[74] These differences in brain function, as well as differences in global symptom network strengths also explain the different manifestations in *loss of pleasure* and *weight/appetite loss* between the two anhedonic subtypes.

However, *weight/appetite loss* in melancholic subtypes may also be involved in other neural correlations. Consistent with previous findings on the neural correlates of weight/appetite changes,[75–77] we found that *weight/appetite loss* in melancholic subtypes was associated with the fALFF value of the praecuneus, which was involved in self-referential processing.[78] Although speculative, reduced spontaneous activity in the praecuneus may potentially be linked to a diminished awareness of internal bodily signals of hunger[75] due to the fact that patients with melancholic MDD tend to have a ruminative focus on sad mood.[79] Brain function alterations in these two melancholic depression subtypes were mainly observed in the default mode network (DMN) and the subcortical network, involving emotional processing. In addition, we uncovered the difference in ALFF values

between the two melancholic depression subtypes in the right temporal pole/parahippocampal gyrus, which is a part of the affective network[80] and has been proven to be closely associated with anxiety symptoms.[81] Spontaneous neural activity differences in these regions explained the difference in *feeling anxious* between the two melancholic subtypes. Meanwhile, brain activity involving the reward function also contributed to the difference in *loss of pleasure* between the two melancholic subtypes.

The definition of atypical-like depression in the current study was attributable to lower scores on *weight/appetite loss* and *sleep reduction* (close to 0). The atypical-like depression subtype had a significantly different symptom structure compared to the two anhedonic depression subtypes, especially in the associations between *loss of pleasure* and other symptoms (such as *weight/appetite loss*, *sleep reduction*, *worthlessness/guilt*, etc.). We did not find differences in symptom network structure between the melancholic subtype and the atypical-like subtype. In part, this may be due to the fact that we cannot directly measure atypical features, which are the main differences between melancholic and atypical depression subtypes. However, the neuroimaging results supported the distinction of this group from others, suggesting this group may represent those patients with atypical-like features. The brain functional alterations of the atypical-like subtype mainly focus on the FC of the salience/ventral attention network (especially in the insula) and the sensory cortex compared to other subtypes. For example, atypical depression significantly differed from severe melancholic depression in the FC of left frontal operculum/insula-right visual cortex (calcarine/lingual) and differed from moderate anhedonic depression in the FC of right frontal operculum/insula-right somatomotor cortex (pre/postcentral gyrus). The insula is a multimodal integration region that receives afferents from sensory, limbic, autonomic (also referred to as the 'ingestive cortex'), and frontal regions, integrating them to achieve different functions through connections with other systems,[82] including sensorimotor processing, cognitive functioning, and socio-emotional processing.[83] Differences in connectivity of the insula-sensory cortex between atypical-like depression and other subtypes may be associated with its reversed vegetative symptoms (especially for weight/appetite) given the central role of the insula in interoception is therefore key in obesity and associated with both increased sensitivity to hunger signals and decreased sensitivity to satiety signals.[84] The pathway from the insula to the sensory cortex might constitute a neural pathway that is involved in the integration of information pertinent to taste and food-related reward processing. For instance, the FC of the left frontal operculum/insula-right visual cortex significantly correlated with *weight/appetite loss*, suggesting that the higher the FC, the more severe the *weight/appetite loss*. Moreover, atypical-like depression also showed decreased FCs involved in reward-related regions (e.g., caudate, nucleus accumbens, and globus pallidus) compared with HC (refer to Suppl. eFigure S8). These reward-related FC abnormalities cannot be explained by *loss of pleasure*. Previous studies suggested that abnormalities in the reward system may underlie the clinical phenomenon of atypical MDD, while the abnormal reward function in atypical-like depression is characterised by abnormal reward sensitivity (e.g., increased sensitivity to food cues) rather than a blunted reward response that underlies anhedonia.[85,86] Therefore, the consistency of symptom profiles and neuroimaging findings suggests that this group may be a subset of patients with atypical-like features. Further validation is warranted to re-evaluate the presence of this subtype by directly measuring atypical features.

It should be noted that due to the uneven distribution of the five subtypes obtained based on the data-driven method, the imbalanced sample sizes between the identified subtypes and between each subtype and HC may introduce potential bias regarding the findings derived from group comparisons, such as reduced statistical power (type II error) or skewed comparisons (where larger groups dominate and distort conclusions about smaller subgroups). Therefore, these results should be interpreted with caution. It may also reflect the natural distribution of MDD subtypes in the patient population. Nonetheless, as the current findings had undergone rigorous statistical corrections, especially for the neural activity findings (both multiple comparison corrections at the whole-brain level and the group level), the present study provides robust results. The differences that survived such stringent corrections likely represent the most distinctive neural activity patterns among the identified subtypes. These observed differences in symptom network structure and neural activity further support the actual existence and the validity of the identified five subtypes in this study.

As previously noted, there have been a number of studies conducted to parse out the heterogeneity of depression by using a data-driven approach. Maglanoc et al. (2019) used high-dimensional data-driven clustering based on depressive and anxiety symptoms to cluster the potential subgroups of depression and compared their symptom centrality and brain functional connectivity between subgroups.[11] They identified five subgroups in terms of symptom severity and the number of subjects with and without a history of depression, but did not include those with severe MDD, limiting the generalisability of the subtypes. Three other studies identified biotypes of MDD based on fMRI. Liang et al. (2020)[34] identified two MDD biotypes with differing FC profiles of DMN exhibiting increased and decreased connectivity of DMN (hyperDMN and hypoDMN), respectively. However, they did not find significant differences in terms of demographic and clinical variables

between the two biotypes. Drysdale et al.[22] and Dunlop et al.[33] have employed commendable work in this field, and promising results have been achieved. Drysdale et al. (2017)[22] discovered four biotypes by using fMRI and these four biotypes with distinct patterns of dysfunctional connectivity in limbic and frontostriatal networks. These biotypes were associated with unique clinical symptom profiles and were also predictive of responsiveness to transcranial magnetic stimulation therapy, highlighting the potential clinical significance of such subgrouping. Recently, Dunlop et al. (2024) also identified 3 robust and generalisable brain-behaviour dimensions using resting-state fMRI that explained individual differences in depressed mood and anxiety, anhedonia, and insomnia, indicating four biotypes of depression.[33] These two studies provide valid findings and hold promise for their potential clinical value. In fact, as Stoyanov et al.[87] explained, in recent years, the nomothetic network psychiatry paradigm (NNP) based on high-dimensional data (such as multimodal neuroimaging and molecular data) has provided an innovative and comprehensive framework for psychiatric classification. These machine learning-based studies provide more opportunities for both the differential diagnosis of MDD from HC[87] and the resolution of heterogeneity in MDD.[22,33,34] However, challenges are the difficulty in obtaining individual-level MRI data and the high costs associated with acquiring such data for identifying depression subtypes. Consequently, clinicians may not be able to directly benefit from the findings of MDD biotypes in their practice. Our study is not positioned as a competing approach to NNP but rather as a complementary effort. By identifying symptom subtypes through LPA, future studies could also integrate these findings with NNP methodologies to examine how clinic-biological markers map onto symptom-defined subtypes. In other words, the added value of this study includes contributing to the literature of the identified subtypes with distinct symptom patterns and their unique associated neural activity alterations, and its incremental value to clinical practice. Clinicians can use easily accessible standard DSM depressive symptoms combined with the model generated by the current study, to identify a patient's subtype and provide targeted and specialised treatments by focussing on relevant therapeutic targets based on the information provided by neuroimaging characteristics of each subtype, thereby helping to achieve optimal personalised treatments.

Future directions, strengths, and limitations

The results of this study offer the possibility for integrating the parsing of MDD heterogeneity with clinical practice even if it is a preliminary attempt. We used validated clinically measured depressive symptoms from DSM-5 that could help to address the challenges of clinical implementation faced by prior studies that have made it difficult to translate research findings into real-world applications. Secondly, we adopted rigorous methodological methods and employed a relatively large sample of neuroimaging data to re-validate the actual existence of these subtypes both at the symptomatology (symptom structures) and neurophysiology (neural activity profiles) levels. The associations between the core symptoms of certain subtypes and specific neural activities were discovered. The consistent findings across different approaches and fields increase the credibility of our findings and suggest their promising implications in clinical settings, which may facilitate the implementation of precision and individualised treatment for depression. Future research is warranted to replicate the characterisation of MDD subtypes. This study would also benefit from developing a user-friendly interface to ease the characterisation of subtypes at the individual level. Once possible clinical subtypes are identified, targeted and specialised intervention and treatment focussing on relevant therapeutic targets based on the neuroimaging characteristics of each subtype could help to yield optimal treatment outcomes. For example, the treatment for anhedonic depression may benefit from selecting therapy targeting reward function (e.g., NMDA Antagonists[88] or targeted psychological interventions such as Positive Affect Treatment[89]); the treatment for atypical depression may benefit from selecting therapy that targets the somatomotor cortex. This aligns with previous studies indicating that atypical depression presented a distinct motor cortical excitability pattern of decreased cortical inhibition and increased cortical facilitation,[90] and responded better to monoamine oxidase inhibitors.[91] Likewise, the melancholic depression treatment may be enhanced by antidepressants that could normalise connectivity between the DMN and mood regulatory networks (e.g., ketamine, escitalopram).[92] Additionally, other symptom differences should also be considered in the context of clinical management, such as higher anxiety in moderate melancholic depression but lower in severe melancholic depression. Despite the promising clinical relevance of our study, further research is needed to ascertain the accuracy of MDD subtyping.

Several limitations are to be noted. First, the classification of atypical depression should be further evaluated as the current study did not have direct measures of atypical features. Second, the cross-sectional nature of this study cannot infer the stability of these subtypes over time and their response to treatment. Longitudinal studies are warranted to test the transition of MDD subtypes and their response to treatment over time. Third, the current study was drawn from a Chinese population of patients with MDD. The generalisability of the identified MDD subtypes needs to be validated in other populations given that the ethnocultural differences may impact MDD clinical manifestations.

The current study employed robust data-driven approaches to unveil five distinct MDD subtypes. The reproducibility of the classification was confirmed in an independent dataset, and the validity of these subtypes was supported by symptomatology (symptom structure) and neurophysiology (neural activity). Notably, each subtype was associated with core symptoms that exhibited specific connections to brain function within certain brain regions. Tailored treatment and management strategies focussing on core symptoms of these subtypes might benefit patients with different MDD subtypes.

Contributors

Xiang Wang: Investigation, Data curation, Formal analysis, Writing - original draft. Yingying Su: Methodology, Formal analysis, Writing - review & editing. Qian Liu: Investigation, Writing - review & editing. Muzi Li: Methodology, Writing - review & editing. Yashar Zeighami: Methodology, Writing - review & editing. Jie Fan: Investigation, Writing - review & editing. G. Camelia Adams: Writing - review & editing. Changlian Tan: Resources, Supervision. Xiongzhao Zhu: Supervision, Funding acquisition, Writing - review & editing. Xiangfei Meng: Conceptualisation, Supervision, Writing - review & editing. Xiang Wang, Xiongzhao Zhu, and Xiangfei Meng have accessed and verified the underlying data. All authors read and approved the final version of the manuscript.

Data sharing statement

The data and code that support the findings of the study are available in Github repository (https://github.com/Xiang-Wangs/MDD-Subtyping.git) for the purpose of transparency. The dataset is shared under a restricted usage policy and may not be used for any additional research or public dissemination without prior approval from the authors. Any use of the data for purposes other than replication of the published results requires explicit consent from the corresponding authors.

Declaration of interests

All of authors declare no competing interests.

Acknowledgements

This work was supported by the Fundamental Research Funds for the National Natural Science Foundation of China (Xiongzhao Zhu, grant number 82171532), and the State Scholarship Fund from China Scholarship Council (CSC) (Xiang Wang, award number 202206370187). We are grateful for the generosity of time and effort by all the participants, and all the researchers who make this project possible.

Appendix A. Supplementary data

Supplementary data related to this article can be found at https://doi.org/10.1016/j.ebiom.2025.105756.

References

1 Lynall ME, McIntosh AM. The heterogeneity of depression. *Am J Psychiatry*. 2023;180(10):703–704.
2 Pitsillou E, Bresnehan SM, Kagarakis EA, et al. The cellular and molecular basis of major depressive disorder: towards a unified model for understanding clinical depression. *Mol Biol Rep*. 2020;47(1):753–770.
3 Beijers L, Wardenaar KJ, van Loo HM, Schoevers RA. Data-driven biological subtypes of depression: systematic review of biological approaches to depression subtyping. *Mol Psychiatry*. 2019;24(6):888–900.
4 Simon GE, Perlis RH. Personalized medicine for depression: can we match patients with treatments? *Am J Psychiatry*. 2010;167(12):1445–1455.
5 Trivedi MH. Right patient, right treatment, right time: biosignatures and precision medicine in depression. *World Psychiatry*. 2016;15(3):237–238.
6 Korte SM, Prins J, Krajnc AM, et al. The many different faces of major depression: it is time for personalized medicine. *Eur J Pharmacol*. 2015;753:88–104.
7 Maj M, Stein DJ, Parker G, et al. The clinical characterization of the adult patient with depression aimed at personalization of management. *World Psychiatry*. 2020;19(3):269–293.
8 Lamers F, de Jonge P, Nolen WA, et al. Identifying depressive subtypes in a large cohort study: results from the Netherlands Study of Depression and Anxiety (NESDA). *J Clin Psychiatry*. 2010;71(12):1582–1589.
9 Schotte CK, Maes M, Cluydts R, Cosyns P. Cluster analytic validation of the DSM melancholic depression. The threshold model: integration of quantitative and qualitative distinctions between unipolar depressive subtypes. *Psychiatry Res*. 1997;71(3):181–195.
10 Maes M, Maes L, Schotte C, Cosyns P. A clinical and biological validation of the DSM-III melancholia diagnosis in men: results of pattern recognition methods. *J Psychiatr Res*. 1992;26(3):183–196.
11 Maglanoc LA, Landrø NI, Jonassen R, et al. Data-driven clustering reveals a link between symptoms and functional brain connectivity in depression. *Biol Psychiatry Cogn Neurosci Neuroimaging*. 2019;4(1):16–26.
12 Maes M, Cosyns P, Maes L, D'Hondt P, Schotte C. Clinical subtypes of unipolar depression: Part I. A validation of the vital and nonvital clusters. *Psychiatry Res*. 1990;34(1):29–41.
13 Milaneschi Y, Lamers F, Mbarek H, Hottenga JJ, Boomsma DI, Penninx BW. The effect of FTO rs9939609 on major depression differs across MDD subtypes. *Mol Psychiatry*. 2014;19(9):960–962.
14 Yu C, Arcos-Burgos M, Licinio J, Wong ML. A latent genetic subtype of major depression identified by whole-exome genotyping data in a Mexican-American cohort. *Transl Psychiatry*. 2017;7(5):e1134.
15 Gibbons RD, Davis JM. Consistent evidence for a biological subtype of depression characterized by low CSF monoamine levels. *Acta Psychiatr Scand*. 1986;74(1):8–12.
16 Åsberg M, Thorén P, Traskman L, Bertilsson L, Ringberger V. "Serotonin depression"—a biochemical subgroup within the affective disorders? *Science*. 1976;191(4226):478–480.
17 Westenberg HG, Verhoeven WM. CSF monoamine metabolites in patients and controls: support for a bimodal distribution in major affective disorders. *Acta Psychiatr Scand*. 1988;78(5):541–549.
18 Feighner JP, Sverdlov L, Nicolau G, Noble JF. Cluster analysis of clinical data to identify subtypes within a study population following treatment with a new pentapeptide antidepressant. *Int J Neuropsychopharmacol*. 2000;3(3):237–242.
19 Ballard ED, Yarrington JS, Farmer CA, et al. Characterizing the course of suicidal ideation response to ketamine. *J Affect Disord*. 2018;241:86–93.
20 Price RB, Lane S, Gates K, et al. Parsing heterogeneity in the brain connectivity of depressed and healthy adults during positive mood. *Biol Psychiatry*. 2017;81(4):347–357.
21 Price RB, Gates K, Kraynak TE, Thase ME, Siegle GJ. Data-driven subgroups in depression derived from directed functional connectivity paths at rest. *Neuropsychopharmacology*. 2017;42(13):2623–2632.
22 Drysdale AT, Grosenick L, Downar J, et al. Resting-state connectivity biomarkers define neurophysiological subtypes of depression. *Nat Med*. 2017;23(1):28–38.
23 Cheng Y, Xu J, Yu H, et al. Delineation of early and later adult onset depression by diffusion tensor imaging. *PLoS One*. 2014;9(11):e112307.
24 Feder S, Sundermann B, Wersching H, et al. Sample heterogeneity in unipolar depression as assessed by functional connectivity analyses is dominated by general disease effects. *J Affect Disord*. 2017;222:79–87.
25 Gold P, Chrousos G. Organization of the stress system and its dysregulation in melancholic and atypical depression: high vs low CRH/NE states. *Mol Psychiatry*. 2002;7(3):254–275.
26 Lewy AJ, Lefler BJ, Emens JS, Bauer VK. The circadian basis of winter depression. *Proc Natl Acad Sci U S A*. 2006;103(19):7414–7419.
27 Schatzberg AF, Posener JA, DeBattista C, Kalehzan BM, Rothschild AJ, Shear PK. Neuropsychological deficits in psychotic versus nonpsychotic major depression and no mental illness. *Am J Psychiatry*. 2000;157(7):1095–1100.

28 Trombello JM, Pizzagalli DA, Weissman MM, et al. Characterizing anxiety subtypes and the relationship to behavioral phenotyping in major depression: results from the EMBARC study. *J Psychiatr Res*. 2018;102:207–215.
29 Benazzi F. Agitated depression: a valid depression subtype? *Prog Neuropsychopharmacol Biol Psychiatry*. 2004;28(8):1279–1285.
30 Lynch CJ, Gunning FM, Liston C. Causes and consequences of diagnostic heterogeneity in depression: paths to discovering novel biological depression subtypes. *Biol Psychiatry*. 2020;88(1):83–94.
31 Thase ME. Recognition and diagnosis of atypical depression. *J Clin Psychiatry*. 2007;68(Suppl 8):11–16.
32 Tokuda T, Yoshimoto J, Shimizu Y, et al. Identification of depression subtypes and relevant brain regions using a data-driven approach. *Sci Rep*. 2018;8(1):14082.
33 Dunlop K, Grosenick L, Downar J, et al. Dimensional and categorical solutions to parsing depression heterogeneity in a large single-site sample. *Biol Psychiatry*. 2024;96(6):422–434.
34 Liang S, Deng W, Li X, et al. Biotypes of major depressive disorder: neuroimaging evidence from resting-state default mode network patterns. *Neuroimage Clin*. 2020;28:102514.
35 Oldfield RC. The assessment and analysis of handedness: the Edinburgh inventory. *Neuropsychologia*. 1971;9(1):97–113.
36 Sha Z, Pepe A, Schijven D, et al. Handedness and its genetic influences are associated with structural asymmetries of the cerebral cortex in 31,864 individuals. *Proc Natl Acad Sci U S A*. 2021;118(47):e2113095118.
37 Zhang S, Zhou J, Cui J, et al. Effects of 12-week escitalopram treatment on resting-state functional connectivity of large-scale brain networks in major depressive disorder. *Hum Brain Mapp*. 2023;44(6):2572–2584.
38 Ye Y, Wang C, Lan X, et al. Abnormal amygdala functional connectivity in MDD patients with insomnia complaints. *Psychiatry Res Neuroimaging*. 2023;328:111578.
39 Gao F, Fan J, Xia J, et al. Decreased sensitivity to risk levels in ventral stratum in major depressive disorder during risky decision-making. *J Affect Disord*. 2021;282:187–193.
40 Gong Y. Revision of wechsler's adult intelligence scale in China. *Acta Psychol Sin*. 1983;15(3):362–370. https://psycnet.apa.org/record/1984-22187-001.
41 American Psychiatric Association. *Diagnostic and Statistical Manual of Mental Disorders, Fifth Edition: DSM-5*. Washington, DC: American Psychiatric Association; 2013.
42 Braund TA, Palmer DM, Williams LM, Harris AWF. Dimensions of anxiety in Major depressive disorder and their use in predicting antidepressant treatment outcome: an iSPOT-D report. *Psychol Med*. 2020;50(6):1032–1042.
43 Ten Have M, Lamers F, Wardenaar K, et al. The identification of symptom-based subtypes of depression: a nationally representative cohort study. *J Affect Disord*. 2016;190:395–406.
44 Chao-Gan Y, Yu-Feng Z. DPARSF: a MATLAB toolbox for "pipeline" data analysis of resting-state fMRI. *Front Syst Neurosci*. 2010;4:13.
45 Zang YF, He Y, Zhu CZ, et al. Altered baseline brain activity in children with ADHD revealed by resting-state functional MRI. *Brain Dev*. 2007;29(2):83–91.
46 Zou QH, Zhu CZ, Yang Y, et al. An improved approach to detection of amplitude of low-frequency fluctuation (ALFF) for resting-state fMRI: fractional ALFF. *J Neurosci Methods*. 2008;172(1):137–141.
47 Zang Y, Jiang T, Lu Y, He Y, Tian L. Regional homogeneity approach to fMRI data analysis. *Neuroimage*. 2004;22(1):394–400.
48 Jenkinson M, Bannister P, Brady M, Smith S. Improved optimization for the robust and accurate linear registration and motion correction of brain images. *Neuroimage*. 2002;17(2):825–841.
49 Yan CG, Cheung B, Kelly C, et al. A comprehensive assessment of regional variation in the impact of head micromovements on functional connectomics. *Neuroimage*. 2013;76:183–201.
50 Power JD, Barnes KA, Snyder AZ, Schlaggar BL, Petersen SE. Spurious but systematic correlations in functional connectivity MRI networks arise from subject motion. *Neuroimage*. 2012;59(3):2142–2154.
51 Schaefer A, Kong R, Gordon EM, et al. Local-global parcellation of the human cerebral cortex from intrinsic functional connectivity MRI. *Cereb Cortex*. 2018;28(9):3095–3114.
52 Xiao Y, Gilmore G, Kai J, Lau JC, Peters T, Khan AR. A population-averaged structural connectomic brain atlas dataset from 422 HCP-aging subjects. *Data Brief*. 2023;50:109513.
53 Sinha P, Calfee CS, Delucchi KL. Practitioner's guide to latent class analysis: methodological considerations and common pitfalls. *Crit Care Med*. 2021;49(1):e63–e79.
54 Brusco MJ, Shireman E, Steinley D. A comparison of latent class, K-means, and K-median methods for clustering dichotomous data. *Psychol Methods*. 2017;22(3):563–580.
55 Spurk D, Hirschi A, Wang M, Valero D, Kauffeld S. Latent profile analysis: a review and "how to" guide of its application within vocational behavior research. *J Vocat Behav*. 2020;120:103445.
56 Vermunt JK, Magidson J. Latent class cluster analysis. In: Hagenaars JA, McCutcheon AL, eds. *Applied Latent Class Analysis*. Cambridge: Cambridge University Press; 2002:89–106.
57 Lukočienė O, Varriale R, Vermunt JK. The simultaneous decision(s) about the number of lower- and higher-level classes in multilevel latent class analysis. *Sociol Methodol*. 2010;40:247–283.
58 Orsel S, Karadag H, Turkcapar H, Kahilogullari AK. Diagnosis and classification subtyping of depressive disorders: comparison of three methods. *Klin Psikofarmakol Bul Bull Clin Psychopharmacol*. 2010;20(1):57–65.
59 Kohler S, Chrysanthou S, Guhn A, Sterzer P. Differences between chronic and nonchronic depression: systematic review and implications for treatment. *Depress Anxiety*. 2019;36(1):18–30.
60 Borsboom D, Cramer AO. Network analysis: an integrative approach to the structure of psychopathology. *Annu Rev Clin Psychol*. 2013;9:91–121.
61 Epskamp S, Borsboom D, Fried EI. Estimating psychological networks and their accuracy: a tutorial paper. *Behav Res Methods*. 2018;50(1):195–212.
62 Bringmann LF, Elmer T, Epskamp S, et al. What do centrality measures measure in psychological networks? *J Abnorm Psychol*. 2019;128(8):892–903.
63 Zhou J, Liu S, Mayes TL, et al. The network analysis of depressive symptoms before and after two weeks of antidepressant treatment. *J Affect Disord*. 2022;299:126–134.
64 Van Borkulo CD, van Bork R, Boschloo L, et al. Comparing network structures on three aspects: a permutation test. *Psychol Methods*. 2023;28(6):1273–1285.
65 Spisak T, Spisak Z, Zunhammer M, et al. Probabilistic TFCE: a generalized combination of cluster size and voxel intensity to increase statistical power. *Neuroimage*. 2019;185:12–26.
66 Xiang YT, Wang G, Hu C, et al. Demographic and clinical features and prescribing patterns of psychotropic medications in patients with the melancholic subtype of major depressive disorder in China. *PLoS One*. 2012;7(6):e39840.
67 Xin LM, Chen L, Su YA, et al. Prevalence and clinical features of atypical depression among patients with major depressive disorder in China. *J Affect Disord*. 2019;246:285–289.
68 Lin J, Su Y, Rizvi SJ, et al. Define and characterize the anhedonia in major depressive disorder: an explorative study. *J Affect Disord*. 2022;313:235–242.
69 Der-Avakian A, Markou A. The neurobiology of anhedonia and other reward-related deficits. *Trends Neurosci*. 2012;35(1):68–77.
70 Coccurello R. Anhedonia in depression symptomatology: appetite dysregulation and defective brain reward processing. *Behav Brain Res*. 2019;372:112041.
71 Rizvi SJ, Pizzagalli DA, Sproule BA, Kennedy SH. Assessing anhedonia in depression: potentials and pitfalls. *Neurosci Biobehav Rev*. 2016;65:21–35.
72 van Heukelum S, Mars RB, Guthrie M, et al. Where is cingulate cortex? A cross-species view. *Trends Neurosci*. 2020;43(5):285–299.
73 Huerta CI, Sarkar PR, Duong TQ, Laird AR, Fox PT. Neural bases of food perception: coordinate-based meta-analyses of neuroimaging studies in multiple modalities. *Obesity (Silver Spring)*. 2014;22(6):1439–1446.
74 Nusslock R, Alloy LB. Reward processing and mood-related symptoms: an RDoC and translational neuroscience perspective. *J Affect Disord*. 2017;216:3–16.
75 Lepping RJ, Bruce AS, Francisco A, et al. Resting-state brain connectivity after surgical and behavioral weight loss. *Obesity (Silver Spring)*. 2015;23(7):1422–1428.
76 Chen Y, Yu R, DeSouza JFX, et al. Differential responses from the left postcentral gyrus, right middle frontal gyrus, and precuneus to meal ingestion in patients with functional dyspepsia. *Front Psychiatry*. 2023;14:1184797.
77 Yan M, Chen J, Liu F, et al. Disrupted regional homogeneity in major depressive disorder with gastrointestinal symptoms at rest. *Front Psychiatry*. 2021;12:636820.

78 Cavanna AE, Trimble MR. The precuneus: a review of its functional anatomy and behavioural correlates. *Brain*. 2006;129(Pt 3):564–583.
79 Berman MG, Peltier S, Nee DE, Kross E, Deldin PJ, Jonides J. Depression, rumination and the default network. *Soc Cogn Affect Neurosci*. 2011;6(5):548–555.
80 Zeng LL, Shen H, Liu L, et al. Identifying major depression using whole-brain functional connectivity: a multivariate pattern analysis. *Brain*. 2012;135(Pt 5):1498–1507.
81 Li W, Cui H, Zhu Z, et al. Aberrant functional connectivity between the amygdala and the temporal Pole in drug-free generalized anxiety disorder. *Front Hum Neurosci*. 2016;10:549.
82 Gogolla N. The insular cortex. *Curr Biol*. 2017;27(12):R580–R586.
83 Uddin LQ, Nomi JS, Hebert-Seropian B, Ghaziri J, Boucher O. Structure and function of the human insula. *J Clin Neurophysiol*. 2017;34(4):300–306.
84 Milaneschi Y, Simmons WK, van Rossum EF, Penninx BW. Depression and obesity: evidence of shared biological mechanisms. *Mol Psychiatry*. 2019;24(1):18–33.
85 Guo Z-P, Chen L, Tang L-R, et al. The differential orbitofrontal activity and connectivity between atypical and typical major depressive disorder. *Neuroimage Clin*. 2025;45:103717.
86 Piccolo M, Belleau EL, Holsen LM, et al. Alterations in resting-state functional activity and connectivity for major depressive disorder appetite and weight disturbance phenotypes. *Psychol Med*. 2023;53(10):4517–4527.
87 Stoyanov D, Khorev V, Paunova R, et al. Resting-state functional connectivity impairment in patients with major depressive episode. *Int J Environ Res Public Health*. 2022;19(21):14045.
88 Pizzagalli DA. Toward a better understanding of the mechanisms and pathophysiology of anhedonia: are we ready for translation? *Am J Psychiatry*. 2022;179(7):458–469.
89 Craske MG, Meuret AE, Ritz T, Treanor M, Dour H, Rosenfield D. Positive affect treatment for depression and anxiety: a randomized clinical trial for a core feature of anhedonia. *J Consult Clin Psychol*. 2019;87(5):457–471.
90 Veronezi BP, Moffa AH, Carvalho AF, et al. Evidence for increased motor cortical facilitation and decreased inhibition in atypical depression. *Acta Psychiatr Scand*. 2016;134(2):172–182.
91 Shulman KI, Herrmann N, Walker SE. Current place of monoamine oxidase inhibitors in the treatment of depression. *CNS Drugs*. 2013;27(10):789–797.
92 Li J, Chen J, Kong W, Li X, Hu B. Abnormal core functional connectivity on the pathology of MDD and antidepressant treatment: a systematic review. *J Affect Disord*. 2022;296:622–634.